MELBOURNE INSTITUTE
Applied Economic & Social Research

Working Paper Series

What's Mine Is Yours: Sovereign Risk Transmission during the European Debt Crisis

Matthew Greenwood-Nimmo
Viet Hoang Nguyen
Yongcheol Shin

Working Paper No. 17/17
July 2017

THE UNIVERSITY OF MELBOURNE
MELBOURNE INSTITUTE

What's Mine Is Yours: Sovereign Risk Transmission during the European Debt Crisis*

Matthew Greenwood-Nimmo[†], Viet Hoang Nguyen[‡] and Yongcheol Shin[§]

[†] Department of Economics, The University of Melbourne

[‡] Melbourne Institute: Applied Economic & Social Research, The University of Melbourne

[§] Department of Economics and Related Studies, University of York

Melbourne Institute Working Paper No. 17/17

July 2017

* We are grateful to Kathryn St John and Catherine Tanuwidjaja for conscientious research assistance. For constructive discussion we thank In Choi, Juan Carlos Cuestas, Renee Fry-McKibbin, Jongsuk Hahn, Jingong Huang, John Hunter, Minjoo Kim, Faek Menla Ali, Barry Rafferty, Chris Skeels, Tomasz Woźniak and Eliza Wu. This paper has benefited from comments raised by participants at the 2015 Conference of the Paul Woolley Centre for the Study of Capital Market Dysfunctionality (Sydney, December 2015), the Australasian Meeting of the Econometric Society (Sydney, July 2016), the 2016 Asian Meeting of the International Finance and Banking Society (Brunei, August 2016), the 2016 KAEA-KIPF Conference (Sejong City, August 2016), the 2016 University of Melbourne Toulouse School of Economics Workshop (Melbourne, December 2016) and by participants at research seminars at Deakin and Sogang Universities and the Universities of Catania and Piraeus. Greenwood-Nimmo acknowledges financial support from the Australian Research Council (Grant Number DE150100708) and the Faculty of Business and Economics at the University of Melbourne. The usual disclaimer applies. For correspondence, email <matthew.greenwood @unimelb.edu.au>.

Melbourne Institute: Applied Economic & Social Research

The University of Melbourne

Victoria 3010 Australia

***Telephone* +61 3 8344 2100**

***Fax* +61 3 8344 2111**

***Email* melb-inst@unimelb.edu.au**

***WWW Address* melbourneinstitute.unimelb.edu.au**

Abstract

We develop an empirical network model to study bilateral sovereign credit risk spillovers during the European debt crisis. We show that the spillover density is typically asymmetric with heavy tails. This confounds efforts to track time-variation in spillover activity using the mean-based summary statistics that are widespread in the literature. Density-based measures — specifically divergence criteria — yield stronger and timelier signals of changes in spillover activity than mean-based measures. This is particularly apparent for sovereign bailouts, which principally affect the tails of the spillover density. Consequently, density-based measures provide valuable additional information about changes in the credit risk environment.

JEL classification: C58, F45, G15, H63

Keywords: Sovereign credit risk, credit default swaps (CDS), network models and connectedness, spillover density, divergence criteria

I. Introduction

The credit risk associated with sovereign debt issued by developed countries has traditionally been negligible, so much so that government bond yields are often used to approximate risk-free interest rates for asset pricing models, among other applications. Although several sovereign defaults and bailouts occurred in the decades prior to the Great Recession of the late 2000s, they were concentrated in emerging markets, including Argentina, Mexico and Russia. This changed with the Great Recession, which resulted in several European sovereign bailouts and a widespread deterioration in the credit risk of many advanced economies, as exemplified by Standard and Poor's downgrade of US federal government debt in 2011. The clustering of sovereign defaults, bailouts and downgrades in both space and time has been a distinctive feature of recent times and has fueled interest in the study of credit risk transmission among sovereigns. Our goal is to model the network of bilateral credit risk spillovers among a group of European sovereigns, to characterise the density of sovereign credit risk spillovers and to study the evolution of the spillover density over time.

In principle, measures of sovereign credit risk — both bond yield spreads and credit default swap (CDS) spreads[1] — should rapidly adjust to reflect idiosyncratic variations in default risk. In practice, however, sovereign credit spreads display marked comovement across countries. It is well documented that a portion of this comovement derives from the dependence of sovereign credit spreads on common factors which capture broad features of the market for sovereign debt, such as marketwide liquidity and the aggregate risk appetite of investors. Using data up to 2010, Longstaff, Pan, Pedersen, and Singleton (2011) show that a single principal component accounts for up to 64% of variation in sovereign CDS spreads. Furthermore, the authors demonstrate that the effect of domestic macroeconomic conditions on the sovereign CDS spread is typically weaker than that of the VIX and of

[1] A sovereign CDS operates like an insurance contract in which a bondholder pays a premium to transfer the default risk of the bond onto the protection seller over a given time-frame. Due both to its liquidity and to the engagement of many well-informed institutional investors, the CDS market is believed to be the main forum for credit risk price discovery (Blanco, Brennan, and Marsh, 2005).

US stock and high yield markets. These important features of the sovereign credit spread data have also been documented in related research by Pan and Singleton (2008), Ang and Longstaff (2013) and Jeanneret (2015), among others.

In addition to the factor structure, a large literature holds that spillovers among sovereign bond markets may contribute to the observed comovement of sovereign credit spreads (e.g. Gande and Parsley, 2005; Alter and Schüler, 2012; Alter and Beyer, 2014). These spillovers may be driven in part by the portfolio management of fixed income investors. This effect is likely to be particularly strong in the Euro area, where the economic and monetary union encourages greater intra-European diversification among European investors (De Santis and Gérard, 2009) and where banks have historically taken substantial sovereign debt positions in the hope of profiting from the convergence of peripheral bond yields to the European core (Acharya and Steffen, 2015). The broader institutional design of the EU may also contribute to sovereign credit risk comovements. Bolton and Jeanne (2011) demonstrate that the combination of financial integration and imperfect fiscal integration in Europe may induce complex interactions among bond markets, while Lane (2012) observes that Europe was ill-equipped to dampen financial shocks in a concerted manner due to the absence of an area-wide buffer mechanism prior to the crisis. On the topic of financial integration, Acharya, Drechsler, and Schnabl (2014) and Brutti and Sauré (2015) show that the exposure of financial institutions domiciled in sovereign a to debt issued by sovereign b introduces an implicit connection between the credit risk of the two sovereigns. If sovereign b defaults and sovereign a is obliged to bail out its banking sector, then sovereign a absorbs a portion of the banks' credit risk, creating an indirect risk spillover from sovereign b to sovereign a.

In normal times, sovereign credit risk spillovers are unlikely to be a cause for concern. However, spillovers may intensify markedly in times of stress, in line with Ang and Bekaert's (2002) observation of increased financial market comovements under adverse conditions. In their seminal paper, Allen and Gale (2000) define financial contagion as an intensification of spillovers beyond that which would be expected in light of fundamentals and exposure to common shocks. Consequently, the development of tools to track spillover activity over time

has the potential to provide an early warning of contagion risks. Billio, Getmansky, Lo, and Pelizzon (2012, p. 555) argue that by carefully monitoring the topology of financial networks, "we stand a better chance of identifying "black swans" when they are still cygnets". The utility of such tools for policymakers is readily apparent, as reflected in the remarks of ECB Vice-President Vítor Constâncio (2012) among others.

Network models provide the natural framework to study bilateral interactions among entities. Such models have risen to prominence in economics and finance in recent years and network structure is increasingly seen as an important determinant of aggregate outcomes (e.g. Leitner, 2005; Acemoglu, Carvalho, Ozdaglar, and Tahbaz-Salehi, 2012; Alter and Schüler, 2012; Billio et al., 2012; Caporin, Pelizzon, Ravazzolo, and Rigobon, 2013; Diebold and Yilmaz, 2009, 2014; Alter and Beyer, 2014; Greenwood-Nimmo, Nguyen, and Rafferty, 2016). The core of a network model is its adjacency matrix, which characterises the pairwise relations (edges) among the entities (vertices) in the system. Billio et al. (2012) propose an approach to the estimation of unweighted directed adjacency matrices based on pairwise Granger causality test statistics. If the adjacency matrix is denoted $\boldsymbol{A}$ and its (i, j)-th element a_{ij}, then $a_{ij} = 1$ if variable j Granger causes variable i and $a_{ij} = 0$ otherwise. Applying their technique to a large sample of hedge funds, banks, broker/dealers, and insurance companies, Billio et al. show that the network is highly dynamic and becomes much more densely interconnected prior to systemic shocks.

A limitation of Billio et al.'s approach is that the adjacency matrix is unweighted, which may obscure valuable information about the relative magnitudes of bilateral spillovers. An alternative framework which addresses this concern has been proposed by Diebold and Yilmaz (2009; 2014, hereafter collectively DY). The DY technique uses forecast error variance decompositions from an underlying vector autoregressive (VAR) model to construct a weighted directed network. In applications to global equity market spillovers and to the linkages among financial institutions, DY argue that an increase in the proportion of the aggregate forecast error variance explained by bilateral spillovers is associated with systemic shocks. Given that it is changes in the *strength* of spillovers which are likely to be of greatest

concern to policymakers, we adopt the DY framework as the foundation of our analysis.

Both Billio et al. and DY advocate the use of rolling sample analysis to track changes in network topography over time. As the number of rolling samples becomes large, such a framework relies critically on a reductive approach to summarise systemwide spillover activity in a simple manner which facilitates comparisons across rolling samples. The summary statistic proposed by DY is the 'spillover index', which is proportional to the mean bilateral spillover. However, many networks have been shown to be scale-free in the sense that their degree distribution follows an asymptotic power law where the number of vertices to which a given vertex is connected follows a Pareto distribution (Albert and Barabási, 2002). Consequently, a small subset of vertices will account for a large proportion of the connections in a typical network, a result which is reflected in many aspects of social science such as Feld's (1991) friendship paradox. Several studies have shown that the weighted degree distribution may also exhibit similar asymmetry (e.g. Tanaka and Aoyagi, 2008). In practice, we find that this is true of DY networks. Based on simulations from a simple VAR(1) data generating process, Figure 1 demonstrates the profound asymmetry of the weighted degree distribution obtained from the DY framework (a detailed summary of the simulation results is provided in Appendix A). In light of this asymmetry, the mean bilateral spillover is likely to be biased and to provide a poor summary of spillover activity.

— Insert Figure 1 here —

Our principal contribution is to develop a framework to characterise the spillover density in its entirety and to monitor its evolution through time in an intuitive manner. Our framework employs kernel density estimation to estimate the density of bilateral spillovers in each rolling sample. We then propose several techniques that can be applied to the sequence of estimated spillover densities in order to monitor the network topography over time. Consequently, our paper follows closely in the spirit of Billio et al. (2012) and represents a useful addition to the toolbox developed by DY. Not only is our approach unbiased in the presence of an asymmetric spillover density but it conveys stronger and more timely signals

of changes in spillover activity than mean-based spillover indices such as that proposed by DY.

We apply our to technique to a large group of European sovereigns over the period January 2nd 2006 to July 27th 2015. Our results reveal that the spillover density is relatively stable prior to the subprime crisis in the sense that its location and shape do not change notably prior to mid 2007. In this period of relative tranquility, the large majority of bilateral spillovers among sovereigns are very weak but there is a small subset of non-negligible spillovers, mostly involving recently acceded states. Consequently, the spillover density is profoundly right skewed in the pre-crisis period and this asymmetry is precisely the behaviour that challenges the use of the mean as a summary statistic. With the outbreak of the subprime crisis, the spillover density shifts rightward and the skew weakens. This process starts in mid-2007 at the time that Bear Stearns ran into difficulties and continues through the bankruptcy of Lehman Brothers in September 2008. Over this period, the signals arising from the mean-based DY spillover index and our suite of density-based measures are similar. However, from late 2008 until mid 2014, the location of the spillover density is relatively stable and the DY spillover index yields little signal. This contrasts markedly with the density-based measures, which rapidly and strongly reflect the unfolding debt crisis in Greece and the ensuing sequence of sovereign bailouts. These events — which were at the heart of the debt crisis — primarily affect the tails of the spillover density, which leads us to conclude that there is a need for density-based spillover measures to complement the established mean-based measures.

This paper proceeds as follows. Section II summarises the DY framework and introduces our approach to characterising the spillover density. Section III contains our main empirical results as well as further results from a raft of robustness exercises. Section IV concludes.

II. Analytical Framework

A. The Approximating Model

We study spillovers of sovereign risk among a group of $i = 1, 2, \ldots, m$ European sovereigns. To measure changes in the expected default risk associated with debt issued by the i-th sovereign in period t, we use the first difference of its CDS spread measured in basis points, denoted x_{it}. Our analysis employs data provided by Markit which relates to US dollar denominated CDS contracts for unsecured sovereign debt with a tenor of 5 years under a complete restructuring clause. Our selection of these specific CDS contract parameters accords with the market conventions documented by Bai and Wei (2012).

For each sovereign, we also include the change in the ten year government bond yield measured in basis points, y_{it}. In addition to risk premia, long-term bond yields convey information about macroeconomic fundamentals, including market-based expectations of the long-term outlook for growth and inflation. For the i-th sovereign, one would expect the risk component of the long-term bond yield to be closely related to the CDS spread, which is already included in the model. Consequently, in the absence of direct measures of macroeconomic fundamentals sampled at daily frequency, the government bond yield provides a valuable proxy after accounting for sovereign credit risk.

Finally, based on Caporin et al. (2013), we include three additional control variables. First, e_t is the first difference of the three-month Euribor, which captures changes in the cost of short-term interbank loans in the Euro area. Second, s_t is the Euribor-EONIA spread. Unlike the Euribor, which is derived from a survey of unsecured *term* lending rates, EONIA (the Euro OverNight Index Average) is based on a survey of unsecured *overnight* rates. Consequently, EONIA is approximately risk-free and so the Euribor-EONIA spread provides a measure of interbank credit risk. Finally, r_t is the first difference of the variance risk premium (VRP) for the Euro Stoxx 50, a common measure of investors' risk appetite. Following the definition proposed by Bollerslev, Tauchen, and Zhou (2009), the VRP is computed as $VRP_t = IV_t - RV_t$, where IV_t is the one-month-ahead option-

implied risk-neutral variance (given by the square of the VSTOXX) and RV_t is the realised variance computed as the sum of squared five minute returns. As noted by Longstaff et al. (2011), such a set of market-determined control variables should summarise a broad array of economic indicators relevant to investors. The Euribor, EONIA and VSTOXX were downloaded from Bloomberg and the realised variance from the Oxford Man Institute. Unit root tests indicate that all series are stationary over our estimation sample (results are available on request).

Following Billio et al. (2012) and DY, the common practice when studying time-variation in spillover activity is to employ rolling regression analysis. Suppose that the length of the full sample is $t = 1, 2, \ldots, T$ and that a window length of $\tau < T$ is selected (the selection of τ in discussed below). Given τ, one estimates VAR models on rolling samples of length τ, each of which is indexed by $r = 1, 2, \ldots, R$ where $R = T - \tau + 1$. To fix notation, we define the $m \times 1$ vectors $\boldsymbol{x}_t = (x_{1t}, x_{2t}, \ldots, x_{mt})'$ and $\boldsymbol{y}_t = (y_{1t}, y_{2t}, \ldots, y_{mt})'$ and the $n \times 1$ vector $\boldsymbol{z}_t = (e_t, s_t, r_t)'$. The $p^{(r)}$-th order reduced form VAR model for $(\boldsymbol{x}_t', \boldsymbol{y}_t', \boldsymbol{z}_t')'$ estimated on the r-th rolling sample may be written as:

$$\begin{pmatrix} \boldsymbol{x}_t \\ \boldsymbol{y}_t \\ \boldsymbol{z}_t \end{pmatrix} = \begin{pmatrix} \boldsymbol{\alpha}_x^{(r)} \\ \boldsymbol{\alpha}_y^{(r)} \\ \boldsymbol{\alpha}_z^{(r)} \end{pmatrix} + \sum_{j=1}^{p^{(r)}} \begin{pmatrix} \boldsymbol{a}_{xx,j}^{(r)} & \boldsymbol{a}_{xy,j}^{(r)} & \boldsymbol{a}_{xz,j}^{(r)} \\ \boldsymbol{a}_{yx,j}^{(r)} & \boldsymbol{a}_{yy,j}^{(r)} & \boldsymbol{a}_{yz,j}^{(r)} \\ \boldsymbol{a}_{zx,j}^{(r)} & \boldsymbol{a}_{zy,j}^{(r)} & \boldsymbol{a}_{zz,j}^{(r)} \end{pmatrix} \begin{pmatrix} \boldsymbol{x}_{t-j} \\ \boldsymbol{y}_{t-j} \\ \boldsymbol{z}_{t-j} \end{pmatrix} + \begin{pmatrix} \boldsymbol{u}_{x,t}^{(r)} \\ \boldsymbol{u}_{y,t}^{(r)} \\ \boldsymbol{u}_{z,t}^{(r)} \end{pmatrix} \tag{1}$$

for $t = r, \ldots, r + \tau - 1$. In common with Greenwood-Nimmo et al. (2016), we select the lag order for the r-th rolling regression, $p^{(r)}$, optimally by minimisation of the Schwarz Information Criterion. This contrasts with many existing applications of the DY method which impose the same lag order in every rolling sample. To simplify the notation that follows, let the total number of variables entering the system be denoted by $d = 2m + n$ and define $\boldsymbol{g}_t = (\boldsymbol{x}_t', \boldsymbol{y}_t', \boldsymbol{z}_t')'$. Now, we may rewrite (1) compactly as:

$$\boldsymbol{g}_t = \boldsymbol{\alpha}^{(r)} + \sum_{j=1}^{p^{(r)}} \boldsymbol{A}_j^{(r)} \boldsymbol{g}_{t-j} + \boldsymbol{u}_t^{(r)} \tag{2}$$

where the regression residuals $\boldsymbol{u}_t^{(r)} = \left(\boldsymbol{u}_{x,t}^{(r)\prime}, \boldsymbol{u}_{y,t}^{(r)\prime}, \boldsymbol{u}_{z,t}^{(r)\prime}\right)' \sim MN\left(\mathbf{0}, \boldsymbol{\Omega}^{(r)}\right)$ and where:

$$\boldsymbol{\alpha}^{(r)} = \begin{pmatrix} \boldsymbol{\alpha}_x^{(r)} \\ \boldsymbol{\alpha}_y^{(r)} \\ \boldsymbol{\alpha}_z^{(r)} \end{pmatrix} \quad , \quad \boldsymbol{A}_j^{(r)} = \begin{pmatrix} \boldsymbol{a}_{xx,j}^{(r)} & \boldsymbol{a}_{xy,j}^{(r)} & \boldsymbol{a}_{xz,j}^{(r)} \\ \boldsymbol{a}_{yx,j}^{(r)} & \boldsymbol{a}_{yy,j}^{(r)} & \boldsymbol{a}_{yz,j}^{(r)} \\ \boldsymbol{a}_{zx,j}^{(r)} & \boldsymbol{a}_{zy,j}^{(r)} & \boldsymbol{a}_{zz,j}^{(r)} \end{pmatrix} \text{ and } \boldsymbol{\Omega}^{(r)} = \begin{pmatrix} \boldsymbol{\omega}_{xx}^{(r)} & \boldsymbol{\omega}_{xy}^{(r)} & \boldsymbol{\omega}_{xz}^{(r)} \\ \boldsymbol{\omega}_{yx}^{(r)} & \boldsymbol{\omega}_{yy}^{(r)} & \boldsymbol{\omega}_{yz}^{(r)} \\ \boldsymbol{\omega}_{zx}^{(r)} & \boldsymbol{\omega}_{zy}^{(r)} & \boldsymbol{\omega}_{zz}^{(r)} \end{pmatrix}$$

with $\boldsymbol{\Omega}^{(r)}$ being positive-definite. Note that we do not make any assumption about the exogeneity of the variables in $\boldsymbol{y}_t$ and/or $\boldsymbol{z}_t$ with respect to those in $\boldsymbol{x}_t$.

B. The Diebold–Yilmaz Framework

Suppressing the vector of intercepts for simplicity and because it is not central to the computation of forecast error variance decompositions, the Wold representation of (2) is:

$$\boldsymbol{g}_t = \sum_{j=1}^{\infty} \boldsymbol{B}_j^{(r)} \boldsymbol{u}_{t-j}^{(r)} \tag{3}$$

where $\boldsymbol{B}_j^{(r)} = \boldsymbol{A}_1^{(r)} \boldsymbol{B}_{j-1}^{(r)} + \boldsymbol{A}_2^{(r)} \boldsymbol{B}_{j-2}^{(r)} + \ldots$, for $j = 1, 2, \ldots$ with $\boldsymbol{B}_0^{(r)} = \boldsymbol{I}_d$ and $\boldsymbol{B}_j^{(r)} = \mathbf{0}$ for $j < 0$ and where the $\boldsymbol{B}_j^{(r)}$'s are square-summable and causal. Following Pesaran and Shin (1998), the generalised forecast error variance decomposition (GVD) at horizon $h = 0, 1, 2, \ldots, H$ is defined with respect to the parameters of (3) as follows:

$$\vartheta_{i \leftarrow j}^{(r,h)} = \frac{\left(\sigma_{u,jj}^{(r)}\right)^{-1} \sum_{\ell=0}^{h-1} \left(\mathbf{e}_i' \boldsymbol{B}_\ell^{(r)} \boldsymbol{\Omega}^{(r)} \mathbf{e}_j\right)^2}{\sum_{\ell=0}^{h-1} \mathbf{e}_i' \boldsymbol{B}_\ell^{(r)} \boldsymbol{\Omega}^{(r)} \boldsymbol{B}_\ell^{(r)\prime} \mathbf{e}_i} \tag{4}$$

for $i, j = 1, \ldots, d$ where $\sigma_{u,jj}^{(r)}$ is the j-th diagonal element of $\boldsymbol{\Omega}^{(r)}$ and $\mathbf{e}_i$ is a $d \times 1$ selection vector whose i-th element is one and whose remaining elements are zero. Consequently, $\vartheta_{i \leftarrow j}^{(r,h)}$ expresses the proportion of the h-step ahead forecast error variance (FEV) of variable i which can be attributed to shocks in the equation for variable j in the r-th rolling sample.

DY were the first to show that GVDs can be used to form a weighted directed network. Abstracting for now from the well-known scaling issue that arises with GVDs when $\boldsymbol{\Omega}^{(r)}$ is

non-diagonal, one may construct the $d \times d$ connectedness matrix for $\boldsymbol{g}_t$ as follows:

$$\mathbb{C}^{(r,h)} = \begin{pmatrix} \vartheta^{(r,h)}_{1\leftarrow 1} & \vartheta^{(r,h)}_{1\leftarrow 2} & \cdots & \vartheta^{(r,h)}_{1\leftarrow d} \\ \vartheta^{(r,h)}_{2\leftarrow 1} & \vartheta^{(r,h)}_{2\leftarrow 2} & \cdots & \vartheta^{(r,h)}_{2\leftarrow d} \\ \vdots & \vdots & \ddots & \vdots \\ \vartheta^{(r,h)}_{d\leftarrow 1} & \vartheta^{(r,h)}_{d\leftarrow 2} & \cdots & \vartheta^{(r,h)}_{d\leftarrow d} \end{pmatrix} \tag{5}$$

where $\mathbb{C}^{(r,h)}$ has the following block structure which is conformable with $\boldsymbol{g}_t = (\boldsymbol{x}_t', \boldsymbol{y}_t', \boldsymbol{z}_t')'$:

$$\mathbb{C}^{(r,h)} = \begin{pmatrix} \boldsymbol{\vartheta}^{(r,h)}_{x\leftarrow x} & \boldsymbol{\vartheta}^{(r,h)}_{x\leftarrow y} & \boldsymbol{\vartheta}^{(r,h)}_{x\leftarrow z} \\ \boldsymbol{\vartheta}^{(r,h)}_{y\leftarrow x} & \boldsymbol{\vartheta}^{(r,h)}_{y\leftarrow y} & \boldsymbol{\vartheta}^{(r,h)}_{y\leftarrow z} \\ \boldsymbol{\vartheta}^{(r,h)}_{z\leftarrow x} & \boldsymbol{\vartheta}^{(r,h)}_{z\leftarrow y} & \boldsymbol{\vartheta}^{(r,h)}_{z\leftarrow z} \end{pmatrix} \tag{6}$$

For a given horizon, h, and a given rolling sample, r, $\underset{(m\times m)}{\boldsymbol{\vartheta}^{(r,h)}_{x\leftarrow x}}$ characterises risk spillovers among the European sovereigns while $\underset{(m\times m)}{\boldsymbol{\vartheta}^{(r,h)}_{x\leftarrow y}}$ and $\underset{(m\times n)}{\boldsymbol{\vartheta}^{(r,h)}_{x\leftarrow z}}$ summarise spillovers from the market-specific economic conditions and the global control variables (respectively) onto sovereign risk. The interpretation of the remaining blocks of $\mathbb{C}^{(r,h)}$ follows easily in a similar fashion.

The approach proposed by Diebold and Yilmaz (2014) is to normalise the (i,j)-th element of $\mathbb{C}^{(r,h)}$ by a factor of $1/\sum_{j=1}^{d} \vartheta^{(r,h)}_{i,j}$ for $i,j = 1,2,\ldots,d$ such that each row of $\mathbb{C}^{(r,h)}$ sums to unity. However, our interest is solely in risk spillovers among the European sovereigns — we include the control variables, $\boldsymbol{y}_t$ and $\boldsymbol{z}_t$, to control for the influence of market-specific conditions and global common factors but spillovers involving the control variables are not our primary interest. Therefore, we apply the DY normalisation to $\boldsymbol{\vartheta}^{(r,h)}_{x\leftarrow x}$ directly — that is, we define the normalised (i,j)-th element of $\boldsymbol{\vartheta}^{(r,h)}_{x\leftarrow x}$ as $\theta^{(r,h)}_{i\leftarrow j} = \vartheta^{(r,h)}_{i\leftarrow j} / \sum_{j=1}^{m} \vartheta^{(r,h)}_{i\leftarrow j}$ for $i,j = 1,2,\ldots,m$. Consequently, we may write the normalised

$m \times m$ block of the h-step ahead connectedness matrix corresponding to spillovers in $\boldsymbol{x}_t$ as:

$$\boldsymbol{\theta}_{x \leftarrow x}^{(r,h)} = \begin{pmatrix} \theta_{1\leftarrow 1}^{(r,h)} & \theta_{1\leftarrow 2}^{(r,h)} & \cdots & \theta_{1\leftarrow m}^{(r,h)} \\ \theta_{2\leftarrow 1}^{(r,h)} & \theta_{2\leftarrow 2}^{(r,h)} & \cdots & \theta_{2\leftarrow m}^{(r,h)} \\ \vdots & \vdots & \ddots & \vdots \\ \theta_{m\leftarrow 1}^{(r,h)} & \theta_{m\leftarrow 2}^{(r,h)} & \cdots & \theta_{m\leftarrow m}^{(r,h)} \end{pmatrix} \tag{7}$$

where $\boldsymbol{\theta}_{x\leftarrow x}^{(r,h)}$ can be thought of as the connectedness matrix for $\boldsymbol{x}_t$ conditional on $\boldsymbol{y}_t$ and $\boldsymbol{z}_t$. Controlling for the influence of market-specific economic conditions and global factors in this way is important if we are to distinguish between true bilateral spillovers of sovereign risk and comovements induced by exposure to common shocks, for example.

C. Accounting for Compositional Changes

Estimation over rolling samples introduces an attendant complication when working with sovereign CDS data — unlike the simple case assumed above, the number of sovereigns in the sample changes through time as the sovereign CDS market broadens considerably during our sample period. Table 1 records how the number of sovereigns in our sample changes over our sample, from 02-Jan-2006 to 27-Jul-2015. At the start of our sample, we have data for 20 sovereigns including most of the major European markets. The significant markets which are missing at this stage are the UK and Switzerland, which are added to the sample in March 2006 and January 2009, respectively. In addition, Bulgaria enters the sample in April 2006. Thus, our largest sample includes 23 sovereigns. Greece is the only sovereign to exit the sample. As a result of its debt crisis, Greek CDS started trading on a points upfront basis and the market became highly illiquid.[2] Greek CDS data is not readily available beyond 08-Mar-2012, when the spread is listed as 37,030.49 basis points. We trim

[2]Points upfront trading is an alternative to operating with a running spread in which the protection buyer pays the protection seller in an ongoing manner through the life of the contract. Points upfront trading involves the payment of the present value of the protection contract (or a fraction thereof) at the start of the trade. This eliminates the risk that the protection seller may be required to pay out before

the Greek data to 14-Feb-2012, the last observation for which the CDS spread is less than 10,000 basis points. Greece subsequently re-enters our sample on 10-Jun-2013.

— Insert Table 1 here —

In light of these compositional changes, the dimension of the VAR model in the r-th rolling sample is not simply d but $d^{(r)} = 2m^{(r)} + n$. This changing dimension does not pose any problems for estimation of the rolling VAR models nor for computation of the connectedness matrix following the DY approach within each rolling sample. However, it does complicate comparisons across rolling samples, as can be easily seen through a simple thought experiment. Suppose that we have data for 20 sovereigns in the r-th rolling sample and for 21 sovereigns in the $(r+1)$-th rolling sample. For simplicity, suppose also that spillover activity is perfectly uniform in both rolling samples — hence, every element of the spillover matrix for the r-th rolling sample is equal to $(1/20) \times 100\% = 5\%$ while the equivalent figure for the $(r+1)$-th rolling sample is $(1/21) \times 100\% \approx 4.75\%$. In the absence of an appropriate adjustment, it would therefore appear that the average spillover is weaker in samples containing more sovereigns.

To ensure that our spillover measures remain comparable across rolling samples, we multiply every element of $\boldsymbol{\theta}_{y \leftarrow y}^{(r,h)}$ by a scale factor such that:

$$s_{i \leftarrow j}^{(r,h)} = \frac{m^{(r)}}{\max\limits_{r \in \{1,\ldots,R\}} (m^{(r)})} \times \theta_{i \leftarrow j}^{(r,h)} \tag{8}$$

This ensures that spillovers in every rolling sample are expressed on the same scale as in the sample with the largest cross-section of sovereigns. Returning to our thought experiment, after applying our adjustment to the r-th rolling sample, we obtain a value of $(20/21) \times (1/20) \times 100\% \approx 4.75\%$ and the spillover matrices from the two rolling samples are now

having received an income from the contract.

measured on the same scale. The final re-scaled sovereign spillover matrix is given by:

$$\mathbb{S}_{x\leftarrow x}^{(r,h)} = \begin{pmatrix} s_{1\leftarrow 1}^{(r,h)} & s_{1\leftarrow 2}^{(r,h)} & \cdots & s_{1\leftarrow m^{(r)}}^{(r,h)} \\ s_{2\leftarrow 1}^{(r,h)} & s_{2\leftarrow 2}^{(r,h)} & \cdots & s_{2\leftarrow m^{(r)}}^{(r,h)} \\ \vdots & \vdots & \ddots & \vdots \\ s_{m^{(r)}\leftarrow 1}^{(r,h)} & s_{m^{(r)}\leftarrow 2}^{(r,h)} & \cdots & s_{m^{(r)}\leftarrow m^{(r)}}^{(r,h)} \end{pmatrix}. \tag{9}$$

The (i,i)-th diagonal element of $\mathbb{S}_{x\leftarrow x}^{(r,h)}$ measures the proportion of the h-step ahead FEV for the i-th sovereign CDS spread in the r-th rolling sample that can be attributed to shocks to the CDS spread for sovereign i itself — this is known as the *own* contribution. Meanwhile, the (i,j)-th off-diagonal element of $\mathbb{S}_{x\leftarrow x}^{(r,h)}$ measures the proportion of the h-step ahead FEV for the i-th sovereign CDS spread in the r-th rolling sample that can be attributed to shocks to the CDS spread for sovereign j — that is, the *risk spillover* from sovereign j to i.

D. Summarising the Bilateral Spillover Density

Given that the number of elements in $\mathbb{S}_{x\leftarrow x}^{(r,h)}$ is quadratically increasing in $m^{(r)}$, reductive methods are needed to summarise spillover activity. DY propose the aggregate spillover index, $S_{x\leftarrow x}^{(r,h)}$:

$$S_{x\leftarrow x}^{(r,h)} = \frac{\boldsymbol{e}'_{m^{(r)}}\mathbb{S}_{x\leftarrow x}^{(r,h)}\boldsymbol{e}_{m^{(r)}} - \text{trace}\left(\mathbb{S}_{x\leftarrow x}^{(r,h)}\right)}{\boldsymbol{e}'_{m^{(r)}}\mathbb{S}_{x\leftarrow x}^{(r,h)}\boldsymbol{e}_{m^{(r)}}} \times 100\% \tag{10}$$

where, due to the scale factor that we introduce in (8):

$$\boldsymbol{e}'_{m^{(r)}}\mathbb{S}_{x\leftarrow x}^{(r,h)}\boldsymbol{e}_{m^{(r)}} = \frac{m^{(r)}}{\max\limits_{r\in\{1,\ldots,R\}}(m^{(r)})} \times m^{(r)}$$

Consequently, it follows that the DY spillover index is proportional to the mean bilateral spillover (i.e. the mean of the off-diagonal elements of $\mathbb{S}_{x\leftarrow x}^{(r,h)}$). To see this, note that:

$$\mathbb{E}\left[s_{i\leftarrow j,j\neq i}^{(r,h)}\right] = \frac{\boldsymbol{e}'_{m^{(r)}}\mathbb{S}_{x\leftarrow x}^{(r,h)}\boldsymbol{e}_{m^{(r)}} - \text{trace}\left(\mathbb{S}_{x\leftarrow x}^{(r,h)}\right)}{m^{(r)}(m^{(r)}-1)} \equiv \frac{S_{x\leftarrow x}^{(r,h)}}{m^{(r)}-1} \times \frac{m^{(r)}}{\max\limits_{r\in\{1,\ldots,R\}}(m^{(r)})} \tag{11}$$

While the mean provides an elementary summary of spillover activity, it only conveys information about the location of the spillover density and not its shape. Furthermore, reliance on the mean may be inappropriate when the spillover density is asymmetric (recall Figure 1). Consequently, measures designed to summarise spillover activity should take account of both the location and the shape of the spillover density.

We proceed by estimating the probability density function of the set of bilateral spillovers $\left\{s_{i\leftarrow j}^{(r,h)}\right\}_{i,j=1,i\neq j}^{m}$ via kernel density estimation (KDE). To this end, we define an $\eta \times 1$ vector of grids, $\boldsymbol{\nu} = (\nu_1, \nu_2, \ldots, \nu_\eta)'$. We follow the established practice and set $\eta = 1,024$. We then estimate the spillover density as:

$$\widehat{g}^{(r,h)}(\nu_l) = \frac{1}{b^{(r,h)}} \left(\frac{1}{m^{(r)}(m^{(r)}-1)} \right) \sum_{i,j=1;i\neq j}^{m^{(r)}} K\left(\frac{\nu_l - s_{i\leftarrow j}^{(r,h)}}{b^{(r,h)}} \right), \; l = 1, 2, \ldots, \eta \tag{12}$$

where K is a kernel and $b^{(r,h)}$ denotes the bandwidth. To ensure that $\widehat{g}^{(r,h)}(\nu_l)$ integrates to unity over the selected range of grid points, we employ the following common normalisation:

$$\widehat{f}^{(r,h)}(\nu_l) = \frac{\widehat{g}^{(r,h)}(\nu_l)}{\text{RSUM}\left(\widehat{\boldsymbol{g}}^{(r,h)}\right)} \tag{13}$$

where $\text{RSUM}\left(\widehat{\boldsymbol{g}}^{(r,h)}\right)$ denotes a numerical Riemann sum of $\widehat{\boldsymbol{g}}^{(r,h)} = \left(\widehat{g}^{(r,h)}(\nu_1), \ldots, \hat{g}^{(r,h)}(\nu_\eta)\right)'$. Given that a variety of kernels are in widespread use in economics and finance, we study how the choice of kernel affects the analysis. We consider four popular kernels: (i) the Gaussian kernel with Silverman's (1986) rule-of-thumb bandwidth; (ii) the Gaussian kernel with the asymptotically optimal bandwidth; (iii) the Epanechnikov kernel with the asymptotically optimal bandwidth; and (iv) the adaptive kernel density estimator of Botev, Grotowski, and Kroese (2010, BGK).

Proceeding in this way, for a chosen kernel and a given window length (τ) and forecast horizon (h) we construct a sequence of $r = 1, 2, \ldots, R$ spillover densities, one for each rolling sample. The next step is to evaluate the evolution of the spillover density over rolling samples. If one wishes to focus on a small subset of the estimated densities, then it

is feasible to directly compare them against one-another or against a suitable benchmark density. This may be a desirable approach if one intends to study specific events. In many cases, however, one may desire a higher frequency characterisation of the evolution of the spillover density which naturally requires a more reductive approach to analysis. A simple solution is to compute a desired set of percentiles or moments for the R densities, each of which may then be treated as a synthetic time series with R observations. A more sophisticated solution is to compare each of the R estimated densities against a desired benchmark density, f_0, using one or more divergence criteria. We consider the following divergence criteria:

$$D_{HN}\left(\widehat{f}^{(r,h)}, f_0\right) = \sup_{\nu} \left|\widehat{f}^{(r,h)}(\nu) - f_0(\nu)\right| \Big/ \sup_{\nu} f_0(\nu) \tag{14}$$

$$D_{KL}\left(\widehat{f}^{(r,h)}, f_0\right) = \int \widehat{f}^{(r,h)}(\nu) \ln\left\{\widehat{f}^{(r,h)}(\nu) \Big/ f_0(\nu)\right\} d\nu \tag{15}$$

where $\widehat{f}^{(r,h)}$ is the estimated density under evaluation. D_{HN} is the Hilbert norm and D_{KL} is the Kullback Leibler Information Criterion (KLIC). Both measures are strictly non-negative and take the value zero only if $\widehat{f}^{(r,h)} = f_0$.[3]

The choice of benchmark density is an important one. In principle, one may define a theoretical benchmark spillover density. This is an intriguing possibility but it is beyond our scope in this paper — we adopt a simpler approach. Given that we are particularly interested in tracing the evolution of the spillover density through time, our suggestion is to treat the estimated density from the first rolling sample as the benchmark — that is to set $f_0 = \widehat{f}^{(1,h)}$. Our first rolling sample spans a period of relative tranquility in the financial markets (02-Jan-2006 to 15-Dec-2006) and so the resulting spillover density can be considered typical for 'normal' times. This proposition is validated in our empirical analysis, where we find that the estimated spillover densities in all rolling samples ending prior to the outbreak of the subprime crisis in mid 2007 are qualitatively and quantitatively similar.

[3]Results for a variety of alternative divergence criteria are available on request.

III. Results

Our first task is to choose an appropriate window length (τ) and forecast horizon (h). While there is no simple method to select either value optimally, the existing literature provides a useful guide. Applications of the DY method to daily data have used a range of values. Diebold and Yilmaz (2014) obtain their main results using $\tau = 100$ and $h = 12$ days, Baruník, Kočenda, and Vácha (2016) use $\tau = 200$ and $h = 10$ days and Greenwood-Nimmo et al. (2016) use $\tau = 250$ and $h = 10$ days. Given this uncertainty, the emergent norm in the literature is to evaluate the sensitivity of the connectedness measures to several candidate window lengths and forecast horizons. Adopting this approach, we experiment with $\tau \in \{200, 250, 300\}$ trading days and $h \in \{5, 10, 15\}$ trading days.[4] Table 2(a) reports the common sample correlation coefficients between the DY spillover indices computed under all pairwise combinations of τ and h over these ranges.

— Insert Table 2 here —

The correlations reported in Table 2(a) are remarkably high, indicating that the results are not driven either by the choice of window length or horizon. In fact, for any given window length, the correlation across different values of the forecast horizon is perfect to three decimal places, which indicates that the GVDs have largely converged to their long-run values within 5 days. This reflects the low degree of serial correlation in our data and is a common finding in the existing literature (e.g. Greenwood-Nimmo et al., 2016). We therefore set $\tau = 250$ and $h = 10$ without loss of generality.

A. Elementary Spillover Measures

Figure 2 plots the DY spillover index, $S_{x \leftarrow x}^{(r,10)}$. The figure reveals a gradual increase in aggregate spillover activity until late 2009, with spillovers accounting for little more than 20% of the 10-days-ahead FEV in the system in late 2006 but reaching more than 80% by

[4] Given the dimension of our VAR model, we consider it imprudent to set $\tau < 200$ trading days.

the time of Lehman Brothers' bankruptcy filing. This increase in spillover activity reflects an intensification of the bilateral interactions among sovereigns rather than the influence of common factors, for which our model explicitly controls following Caporin et al. (2013). A particularly striking feature of the figure is the relative stability of the spillover index from late 2008 to mid 2014 despite several sovereign crises and bailouts at this time. We shall return to this observation shortly.

— Insert Figure 2 here —

An obvious question is how the increase in aggregate spillover activity between the start of our sample (the pre-crisis period) and the height of the debt crisis is distributed over the edges in the network. Consider two rolling samples: (i) the first rolling sample from 02-Jan-2006 to 15-Dec-2006, which assumes a particular importance in our analysis as it will be used as a benchmark for subsequent comparisons; and (ii) the rolling sample covering the period 22-Apr-2010 to 06-Apr-2011, the end of which corresponds to the Portuguese request for activation of the aid mechanism in the midst of the sovereign debt crisis.[5] Figures 3 and 4 report the connectedness matrices for these two rolling samples as heatmaps. To facilitate their interpretation, each heatmap has been clustered using an agglomerative single linkage algorithm.[6] Consequently, the order of the sovereigns differs between Figures 3 and 4. Furthermore, due to changes in the cross-sectional composition of our sample over time, 20 sovereigns are included in Figure 3 and 23 in Figure 4, although the estimated spillover effects in both figures are directly comparable by virtue of the scale factor defined in (8).

— Insert Figures 3 and 4 here —

[5]Our choice of the Portuguese bailout sample as a comparison case is essentially arbitrary — we could use any rolling sample during the sovereign debt crisis period and the principal implications that we highlight below would still hold. Detailed results for other samples are available on request.

[6]This is an iterative 'bottom-up' algorithm. To start, every vertex is considered as a cluster in its own right. In each iteration, the pair of clusters which are closest to one-another are merged into a new cluster. The closeness of two clusters is measured by the single strongest connection which exists between members of those clusters. The algorithm terminates when all vertices are included in a single cluster.

Consulting Figure 3, we find that the large majority of bilateral spillovers are very weak in the pre-crisis period. In fact, with the exception of the pairwise spillovers between Poland and Hungary and between the Netherlands and Austria, the remaining spillovers are mostly negligible. The clustering algorithm draws attention to three groups which can be seen as blocks along the prime diagonal of the connectedness matrix — there is a cluster of Eastern European sovereigns (the Czech Republic, Latvia, Russia, Hungary and Poland), a separate cluster of Northern European and Scandinavian sovereigns (Norway, Sweden, Ireland, Finland, Austria, the Netherlands and Denmark) and a group of Southern European sovereigns (Spain, Italy, Greece and Portugal).

Such spatial clustering is indicative of regional effects on sovereign credit spreads. The Northern and Southern European clusters in Figure 3 align closely with popular notions of the European core and periphery. Hale and Obstfeld (2016) summarise the core–periphery distinction in the years preceding the sovereign debt crisis. They argue that a pattern of heavy borrowing, domestic lending booms and rapid asset price inflation became typical of the peripheral economies at this time, fueled by the low borrowing costs associated with EMU membership. Much of this borrowing was intermediated by financial institutions from the core economies, creating a financial boom in the core at the cost of elevated systemic exposure to peripheral risk. Meanwhile, the common behaviour of the Eastern European sovereigns may be attributed to two phenomena. First, with the exception of Russia, this group acceded to the EU in 2004 and their efforts to integrate with the EU will have strongly affected their bond yields.[7] Second, the deep financial, economic and political linkages among Russia and the Commonwealth of Independent States (CIS) naturally creates a degree of comovement within this group, with Russia playing a leading role (Espinosa-Bowen, Ilahi, and Alturki, 2009).

Figure 4 presents a stark contrast relative to Figure 3. Overall, spillover activity has intensified markedly, although increases are not uniformly distributed over the edges in the

[7] Reininger and Walko (2006) note that Polish and Hungarian bond yields were slow to integrate with the EU, which may partially explain the strong bilateral linkage between these sovereigns in Figure 3.

network. At one extreme, Switzerland stands out for being very weakly connected to the rest of the system. At the other extreme, the European core and peripheral blocks — while still visibly distinct — are now much more strongly connected. The increase in core–periphery spillovers reflects the transmission of credit risk via the network of financial intermediation noted above and documented by Hale and Obstfeld (2016). In addition to core–periphery linkages, the figure reveals strong linkages among peripheral states, especially among Ireland, Portugal and Spain and, to a lesser degree, Italy. Such intra-periphery spillovers were a key concern among many policymakers at the time, as credit risk spillovers among troubled states raise the spectre of sovereign contagion (Alter and Schüler, 2012; Constâncio, 2012; Kalbaska and Gatkowski, 2012). Finally, the Eastern European cluster identified in Figure 3 is still readily apparent and is now joined by a new entrant into the sample, Bulgaria.

B. Density-Based Spillover Measures

Figure 5 plots the estimated spillover density in the first rolling sample, 02-Jan-2006 to 15-Dec-2006. To demonstrate the effect of kernel selection on the estimated density, we present results based on the following four implementations of the KDE: (i) the Gaussian kernel using Silverman's (1986) rule-of-thumb bandwidth; (ii) the Gaussian kernel using the asymptotically optimal bandwidth; (iii) the Epanechnikov kernel using the asymptotically optimal bandwidth; and (iv) the BGK adaptive KDE using the data-driven bandwidth.

— Insert Figure 5 here —

Recall that the off-diagonal elements of the connectedness matrix are FEV shares measured in percent. Therefore, the horizontal axis in Figure 5 measures the strength of bilateral spillover effects in percent. Regardless of which kernel is considered, the estimated density closely fits the spillover histogram. The large majority of the probability mass lies close to zero, reflecting our earlier observation based on Figure 3 that most bilateral spillovers are negligible in normal times. The density exhibits a marked skew, with a long right tail corresponding to the subset of strong spillovers noted above.

Figure 6 plots kernel densities for the rolling sample ending with the Portuguese bailout on 06-Apr-2011. Unlike Figure 5, some differences in the behaviour of the four KDEs are now apparent. The Gaussian kernel using Silverman's rule-of-thumb bandwidth over-estimates the mass in both tails quite considerably. When the asymptotically optimal bandwidth is used, both the Gaussian and Epanechnikov kernels perform relatively well. Interestingly, the gain from the variable bandwidth under the BGK adaptive KDE is negligible. Consequently, in deference to the principle of parsimony, we adopt the simple Gaussian kernel with the optimal bandwidth as our benchmark KDE without loss of generality.

— Insert Figure 6 here —

As of April 2011, the spillover density has moved markedly to the right, with the bulk of the probability mass between 1% and 5% and a well-defined peak a little above 2%. Approximately one-third of the probability mass lies beyond 5%, which corresponds to the strong bilateral interactions within the clusters identified above. Due to these changes in the spillover density during the crisis, we no longer observe such a pronounced right skew, indicating that spillovers that would be considered extremely strong in normal times occur with a relatively high probability in times of crisis. When viewed in this way, it follows that increasing systemic stress will typically be reflected not just in an increase in the mean spillover but also in a reduction in the right skew of the spillover density.

To provide a richer indication of how the spillover density evolves over our sample, Figure 7 plots the spillover CDFs and PDFs for the following events: the benchmark sample; Bernanke's warning of subprime risks in March 2007; the acquisition of Bear Stearns by JP Morgan in March 2008; the bankruptcy of Lehman Brothers in September 2008; the first Greek bailout as well as the Irish, Portuguese and Spanish bailouts which occurred between April 2010 and June 2012; and Greece's failure to uphold its payment schedule to the IMF on 30-Jun-2015. At the start of our sample, the bulk of the probability mass is close to zero — more than three quarters of all bilateral spillovers account for no more than 1% of FEV and almost nine out of ten account for no more than 2% of FEV. The overall picture

is very similar in March 2007, when Bernanke (2007) warned of systemic risks related to government-sponsored mortgage enterprises, less than a week before the delisting of New Century Financial, one of the largest subprime lenders in the US.

— Insert Figure 7 here —

An intensification of sovereign credit risk spillovers is readily apparent at the time of JP Morgan's acquisition of Bear Stearns in March 2008. Six months later, at the time of the failure of Lehman Brothers, just 4 out of 10 bilateral spillovers account for less than 1% of FEV while almost the same proportion account for 2.5% of FEV or more and 1 in 10 bilateral spillovers account for 8% of FEV or more. This strong response of the sovereign credit risk network to the financial crisis is natural in light of the existing literature, which has demonstrated the nexus between financial crises and debt crises and which has shown that Europe was particularly vulnerable to financial shocks due to its institutional design (e.g. Reinhart and Rogoff, 2011; Lane, 2012; Acharya et al., 2014).

Spillovers intensify even further by the time of the first Greek bailout. Just one in six bilateral spillovers is weaker than 1% of FEV at this time, while nearly half of all bilateral spillovers exceed 3% of FEV. To understand the extent to which the spillover density has changed, compare this value to its equivalent in the pre-crisis benchmark sample, where only one in fifteen bilateral spillovers exceeds 3%. In this strongly interconnected environment, an idiosyncratic shock affecting risk in one sovereign is likely to rapidly propagate to others. This fragile regime is sustained throughout several subsequent sovereign bailouts before the spillover density shifts back to the left toward the end of our sample. However, note that the right tail of the spillover density is very heavy at this time, indicating that there is still a substantial concentration of strong spillovers. In practice, these strong spillovers are predominantly bilateral interactions among the GIIPS, which appear to largely decouple from the other sovereigns at this time — it is to this issue that we now turn.

C. Locating Bilateral Spillovers within the Spillover Density

Figure 8 records the strength of bilateral credit risk spillovers among the GIIPS at key times in our sample. The figure covers all of the events addressed in Figure 7 as well as two additional events for Greece — the agreement over the second Greek bailout on 21-Feb-2012 and the Greek debt-swap agreement on 09-Mar-2012. To place the bilateral spillovers in context, we summarise the spillover density corresponding to each event date as a boxplot.

— Insert Figure 8 here —

In the majority of cases, credit risk spillovers among the GIIPS lie in the upper quartile of the spillover density. The strong bilateral transfers of credit risk among the GIIPS suggest that concerns over contagion within this group are well-founded (Constâncio, 2012). The various GIIPS bailouts were motivated in large part by the desire to prevent contagion. It is reasonable to assume that a sustained reduction in outward credit risk spillovers from sovereign i corresponds to a reduction in the contagion risk associated with that sovereign. Figure 8 reveals that some bailouts achieved a sustained reduction in spillover activity. For example, the Portuguese bailout (labelled 'PT' in the figure) occurs when outward spillovers from Portugal are very strong, lying well inside the upper 10% of the spillover density. By the time of the second Greek bailout (labelled 'GR2'), outward spillovers from Portugal are weaker in absolute terms and typically lie more centrally within the spillover density, indicating that the systemic risk posed by Portugal has weakened considerably over this time. Similarly, the first Greek bailout appears to have reduced outward spillovers from Greece and the Irish bailout appears to have reduced spillovers from Ireland to Greece, if not significantly to the other GIIPS states. No such inferences can be drawn for the Spanish bailout based on Figure 8 as the gap between the events 'ES' (the Spanish bailout of June 2012) and 'GRD' (the Greek default on its IMF loan payments in June 2015) is too large. Nonetheless, taken as a whole, our results suggest that sovereign bailouts succeed in reducing outward credit risk spillovers from troubled sovereigns (see also Alter and Beyer, 2014).

The last event that we consider (labelled 'GRD') refers to Greece's failure to meet its IMF loan repayment obligations. This also coincides with the build up to the Greek bailout referendum of 05-Jul-2015, a time of considerable concern over a possible Greek departure from the Eurozone. Figure 8 reveals an unprecedented surge in spillover activity among the GIIPS at this time, which corresponds to the heavy right tail in Figure 7(d). At this time, the risk of political contagion (i.e. the risk of other peripheral states using the Greek precedent in an effort to renegotiate bailout terms subject to the threat that they may otherwise leave the Eurozone) added to the risk of financial contagion, leading to a decoupling of the GIIPS from the other European sovereigns. Similar political risks may feature prominently in the near future in the wake of the Brexit referendum.

D. Rolling Density-Based Spillover Measures

As emphasised by Billio et al. (2012) and DY, if network models are to be useful for monitoring risk, they must be capable of delivering timely signals. Consequently, as a final exercise, we turn our attention to rolling sample analysis of the spillover density. As a precursor, we first verify that our rolling density-based results do not depend critically on the choice of window length or forecast horizon. Table 2(b) reports the balanced sample correlations of the KLIC as we vary $h \in \{5, 10, 15\}$ and $\tau \in \{200, 250, 300\}$. The results reveal somewhat more sensitivity to the choice of forecast horizon than was observed in Table 2(a) using the DY spillover index, although the correlation is never lower than 0.69. Meanwhile, Table 3 compares the performance of the four implementations of the KDE that we consider. The high correlations observed throughout the table indicate that our results are remarkably robust to the choice of KDE. Overall, there is little evidence that the results are sensitive to our modelling choices.

— Insert Table 3 here —

Figure 9 provides a pair of contour plots tracking the spillover histogram and the estimated spillover density over our sample period. The similarity of the two plots indicates

that our KDE approach provides an accurate summary of spillover activity in the system in each rolling sample. The contour plots paint a similar picture as the snapshots in Figure 7, drawing particular attention to the right skew which typically characterises the spillover density. Because of this skew, the mean is typically higher than the median, with the difference between the two reaching approximately 1.5% late in the sample as the GIIPS decouple from the other sovereigns. The stronger the right skew, the more the DY spillover index over-estimates the central tendency of the spillover density. Given that this distortion may often materially affect the interpretation of the results, we recommend that the DY spillover index should be complemented with additional information on the shape of the spillover density. Ideally this can be achieved by presenting the entire spillover density, as in Figure 9. Alternatively, one may pursue a more reductive approach based on a spillover asymmetry measure (SAM). As an illustration, we provide a simple SAM in Figure 9 defined as the difference between the mean and the median, although alternative formulations abound.[8]

— Insert Figure 9 here —

Figure 10 presents a more formal analysis of the dynamic evolution of the spillover density based on the divergence criteria in equations (14) and (15). In each case, we use the first rolling sample to define the benchmark density, f_0. The implicit assumption is that the spillover density at this time is representative of the normal situation in the pre-crisis period. This is supported by the similarity of the spillover densities in the early part of our sample that can be seen in Figure 9. The very low values of both the Hilbert Norm and the KLIC for rolling samples ending in the first half of 2007 suggest that the spillover density for the first sample is indeed representative of the spillover density over this entire period.

— Insert Figure 10 here —

[8]Note that, despite the similar terminology, our spillover asymmetry measure differs from that of Baruník et al. (2016), which is based on a signed decomposition of the variables entering the approximating model.

Both divergence criteria exhibit considerably greater variation than the DY spillover index over the period from late 2008 to mid 2014. Several major events are identified in the figure, including bank failures, sovereign crises, sovereign bailouts and ECB policy interventions. The divergence criteria respond rapidly and strongly to these events. This is also true of the DY index until the failure of Lehman Brothers, after which its response is generally muted. This highlights a distinction between the events of the financial crisis of 2007-8 and the sovereign debt crisis starting in late 2009. Events during the financial crisis are associated with changes in the location of the spillover density — this can be seen clearly in Figure 9 where adverse news relating to Bear Stearns and Lehman Brothers results in step changes in the strength of the mean bilateral spillover. By contrast, the major events of the debt crisis predominantly affect the tails of the spillover density, which explains why the divergence criteria outperform the DY spillover index at this time. This is particularly true of events 'F' and 'G' in Figure 10 which relate to the emergence of the Greek debt crisis and events 'H' to 'M', which relate to bailouts for the GIIPS and Cyprus. In each case, the response of the DY spillover index is mild or negligible but the divergence criteria react strongly.

Our finding that sovereign crises and bailouts mainly affect the tails of the spillover density has an intuitive appeal. These are extreme events which either exacerbate or ameliorate credit risk spillovers and which are likely to have a particularly strong affect on spillovers among the more troubled sovereigns in our sample. In the context of the European debt crisis, it is spillovers among this group that are of primary concern. Indeed, whenever network models are used to model risk transmission, it will typically be the case that the strongest risk spillovers are of the greatest interest. Consequently, measures such as ours which convey information about the shape of the spillover density represent a valuable complement to the mean-based measures which are widely used in the literature at present.

IV. Concluding Remarks

In this paper, we develop an empirical network model to study the evolution of sovereign credit risk spillovers during the European debt crisis. Our approach traces the evolution of the entire spillover density as opposed to focusing solely on its central tendency. This is an important innovation because we demonstrate that the spillover density is typically asymmetric, which confounds efforts to track changes in spillover intensity using established measures which are proportional to the mean bilateral spillover.

Our results reveal that the spillover density is relatively stable prior to the subprime crisis in the sense that its shape does not change notably prior to mid 2007. In this pre-crisis period of relative tranquility, the spillover density is profoundly skewed, with a small subset of strong spillovers standing out among the large majority which are very weak. During the global financial crisis of 2007-8, the spillover density shifts rightward and the skew weakens. Over this period, the signals arising from the mean-based DY spillover index and our suite of density-based measures are similar. By contrast, during the sovereign debt crisis, it is the tails of the spillover density which contain the most information. Consequently, our density-based measures provide much clearer and more timely signals than the DY spillover index at this time. Given that it is the strongest spillovers that populate the right tail of the spillover density which elicit the greatest concern from policymakers, density-based spillover measures represent a valuable complement to the established mean-based measures.

References

Acemoglu, D., V. M. Carvalho, A. Ozdaglar, and A. Tahbaz-Salehi (2012): "The Network Origins of Aggregate Fluctuations," *Econometrica*, 80, 1977–2016.

Acharya, V. V., I. Drechsler, and P. Schnabl (2014): "A Pyrrhic Victory? Bank Bailouts and Sovereign Credit Risk," *Journal of Finance*, 69, 2689–2739.

Acharya, V. V. and S. Steffen (2015): "The "Greatest" Carry Trade Ever? Understanding Eurozone Bank Risks," *Journal of Financial Economics*, 115, 215–236.

Albert, R. and A.-L. Barabási (2002): "Statistical Mechanics of Complex Networks," *Reviews of Modern Physics*, 74, 47–97.

Allen, F. and D. Gale (2000): "Financial Contagion," *Journal of Political Economy*, 108, 1–33.

Alter, A. and A. Beyer (2014): "The Dynamics of Spillover Effects during the European Sovereign Debt Turmoil," *Journal of Banking and Finance*, 42, 134–153.

Alter, A. and Y. S. Schüler (2012): "Credit Spread Interdependencies of European States and Banks During the Financial Crisis," *Journal of Banking and Finance*, 36, 3444–3468.

Ang, A. and G. Bekaert (2002): "International Asset Allocation with Regime Shifts," *Review of Financial Studies*, 15, 1137–1187.

Ang, A. and F. A. Longstaff (2013): "Systemic Sovereign Credit Risk: Lessons from the U.S. and Europe," *Journal of Monetary Economics*, 60, 493–510.

Bai, J. and S.-J. Wei (2012): "When is there a Strong Transfer Risk from the Sovereigns to the Corporates? Property Rights Gaps and CDS Spreads," Working Paper 18600, NBER, Cambridge (MA).

Baruník, J., E. Kočenda, and L. Vácha (2016): "Asymmetric Connectedness on the U.S. Stock Market: Bad and Good Volatility Spillovers," *Journal of Financial Markets*, 27, 55–78.

Bernanke, B. S. (2007): "GSE Portfolios, Systemic Risk, and Affordable Housing," Speech before the Independent Community Bankers of America's Annual Convention and Techworld, Honolulu, Hawaii.

Billio, M., M. Getmansky, A. Lo, and L. Pelizzon (2012): "Econometric Measures of Connectedness and Systemic Risk in the Finance and Insurance Sectors," *Journal of Financial Economics*, 104, 535–559.

Blanco, R., S. Brennan, and I. Marsh (2005): "An Empirical Analysis of the Dynamic Relationship between Investment-Grade Bonds and Credit Default Swaps," *Journal of Finance*, 60, 2255–2281.

Bollerslev, T., G. Tauchen, and H. Zhou (2009): "Expected Stock Returns and Variance Risk Premia," *Review of Financial Studies*, 22, 4463–4492.

Bolton, P. and O. Jeanne (2011): "Sovereign Default Risk and Bank Fragility in Financially Integrated Economies," *IMF Economic Review*, 59, 162–194.

Botev, Z., J. Grotowski, and D. Kroese (2010): "Kernel Density Estimation via Diffusion," *Annals of Statistics*, 38, 2916–2957.

Brutti, F. and P. Sauré (2015): "Transmission of Sovereign Risk in the Euro Crisis," *Journal of International Economics*, 97, 231–248.

Caporin, M., L. Pelizzon, F. Ravazzolo, and R. Rigobon (2013): "Measuring Sovereign Contagion in Europe," Working Paper 18741, NBER, Cambridge (MA).

Constâncio, V. (2012): "Contagion and the European Debt Crisis," *Banque de France Financial Stability Review*, 16, 109–121.

De Santis, R. A. and B. Gérard (2009): "International Portfolio Reallocation: Diversification Benefits and European Monetary Union," *European Economic Review*, 53, 1010–1027.

Diebold, F. and K. Yilmaz (2009): "Measuring Financial Asset Return and Volatility Spillovers, with Application to Global Equity Markets," *Economic Journal*, 119, 158–171.

——— (2014): "On the Network Topology of Variance Decompositions: Measuring the Connectedness of Financial Firms," *Journal of Econometrics*, 182, 119–134.

Espinosa-Bowen, J., N. Ilahi, and F. Alturki (2009): "How Russia Affects the Neighborhood – Trade, Financial, and Remittance Channels," Working Paper 09/277, International Monetary Fund, Washington D.C.

Feld, S. L. (1991): "Why Your Friends Have More Friends Than You Do," *American Journal of Sociology*, 96, 1464–1477.

Gande, A. and D. C. Parsley (2005): "News Spillovers in the Sovereign Debt Market," *Journal of Financial Economics*, 75, 691–734.

Greenwood-Nimmo, M., V. Nguyen, and B. Rafferty (2016): "Risk and Return Spillovers among the G10 Currencies," *Journal of Financial Markets*, in press.

Hale, G. and M. Obstfeld (2016): "The Euro and the Geography of International Debt Flows," *Journal of the European Economic Association*, 14, 115–144.

Jeanneret, A. (2015): "The Dynamics of Sovereign Credit Risk," *Journal of Financial and Quantitative Analysis*, 50, 963–985.

Kalbaska, A. and M. Gatkowski (2012): "Eurozone Sovereign Contagion: Evidence from the CDS Market (2005–2010)," *Journal of Economic Behavior and Organisation*, 83, 657–673.

Lane, P. R. (2012): "The European Sovereign Debt Crisis," *Journal of Economic Perspectives*, 26, 49–67.

Leitner, Y. (2005): "Financial Networks: Contagion, Commitment and Private Sector Bailouts," *Journal of Finance*, 60, 2925–2953.

Longstaff, F., J. Pan, L. Pedersen, and K. Singleton (2011): "How Sovereign Is Sovereign Credit Risk?" *American Economic Journal: Macroeconomics*, 3, 75–103.

Pan, J. and K. J. Singleton (2008): "Default and Recovery Implicit in the Term Structure of Sovereign CDS Spreads," *Journal of Finance*, 63, 2345–2384.

Pesaran, M. and Y. Shin (1998): "Generalized Impulse Response Analysis in Linear Multivariate Models," *Economics Letters*, 58, 17–29.

Reinhart, C. M. and K. S. Rogoff (2011): "From Financial Crash to Debt Crisis," *American Economic Review*, 101, 1676–1706.

Reininger, T. and Z. Walko (2006): "The Integration of Czech, Hungarian and Polish Bond Markets with the Euro Area Bond Market A Déjà-vu of the Club-Med Convergence Plays?" in *Financial Development, Integration and Stability: Evidence from Central, Eastern and South-Eastern Europe*, ed. by K. Liebscher, J. Christl, P. Mooslechner, and D. Ritzberger-Grünwald, Cheltenham: Elgar, chap. 26, 466–488.

Silverman, B. W. (1986): *Density Estimation for Statistics and Data Analysis*, London: Chapman and Hall.

Tanaka, T. and T. Aoyagi (2008): "Weighted Scale-Free Networks with Variable Power-Law Exponents," *Physica D: Nonlinear Phenomena*, 237, 898–907.

Sovereign	ISO Code	Sample Begins	5-year CDS Spreads				10-year Bond Yields			
			Series ID	Mean	Min	Max	Series ID	Mean	Min	Max
Greece	GR	02-Jan-2006	GREECE	4.65	-2455.84	1674.74	S487PL	1.71	-531.96	383.22
Austria	AT	02-Jan-2006	AUST	0.01	-27.49	44.28	S06676	-0.09	-21.70	25.40
Belgium	BE	02-Jan-2006	BELG	0.01	-57.38	35.11	S06040	-0.09	-30.20	34.40
Czech Rep.	CZ	02-Jan-2006	CZECH	0.02	-42.31	46.03	T94667	-0.11	-42.48	43.50
Denmark	DK	02-Jan-2006	DENK	0.01	-15.77	17.60	S05463	-0.10	-28.00	31.18
Finland	FI	02-Jan-2006	FINL	0.01	-8.48	11.82	S06771	-0.10	-23.90	22.30
France	FR	02-Jan-2006	FRTR	0.01	-29.83	23.02	S04538	-0.09	-26.20	24.20
Germany	DE	02-Jan-2006	DBR	0.00	-13.36	11.75	S03258	-0.11	-25.60	18.48
Hungary	HU	02-Jan-2006	REPHUN	0.05	-83.68	125.23	S3099H	-0.14	-95.00	95.00
Iceland	IS	02-Jan-2006	ICELND	0.05	-126.49	279.82	S3099T	-0.04	-336.30	426.90
Ireland	IE	02-Jan-2006	IRELND	0.02	-152.45	113.79	S06033	-0.09	-102.79	75.00
Italy	IT	02-Jan-2006	ITALY	0.04	-74.04	71.80	S05461	-0.06	-78.00	50.90
Lithuania	LT	02-Jan-2006	LITHUN	0.03	-76.87	108.38	S310FK	-0.07	-917.40	915.60
Norway	NO	02-Jan-2006	NORWAY	0.00	-11.88	12.80	S06770	-0.08	-28.27	29.31
Poland	PL	02-Jan-2006	POLAND	0.02	-63.29	55.34	S310KN	-0.09	-75.90	98.10
Portugal	PT	02-Jan-2006	PORTUG	0.06	-167.25	170.66	S03692	-0.03	-146.98	168.60
Russia	RU	02-Jan-2006	RUSSIA	0.11	-168.80	206.86	S310LC	0.17	-299.80	494.80
Spain	ES	02-Jan-2006	SPAIN	0.03	-69.60	59.21	S05462	-0.06	-88.30	37.30
Sweden	SE	02-Jan-2006	SWED	-0.03	-79.33	65.77	S06601	-0.10	-27.51	31.80
Netherlands	NL	02-Jan-2006	NETHRS	0.01	-13.43	25.69	S04540	-0.10	-22.40	17.71
UK	UK	21-Mar-2006	UKIN	0.01	-16.74	17.48	S05358	-0.10	-29.79	26.00
Bulgaria	BG	17-Apr-2006	BGARIA	0.06	-86.22	91.81	S3090X	-0.04	-103.50	91.10
Switzerland	CH	19-Jan-2009	SWISS	-0.04	-43.92	50.20	S05471	-0.12	-21.70	21.94

NOTE: Descriptive statistics are reported for the first difference of each series in basis points. The CDS data are mid-market rates for sovereign debt where the CDS contract has a tenor of 5 years and a cum-restructuring clause. The contrast currency is USD in all cases. The CDS data are sourced from Markit using the series identifiers shown. The 10-year sovereign bond yield data are sourced from Bloomberg using the series identifiers shown.

Table 1: Cross-Sectional Composition of the Estimation Sample, Descriptive Statistics and Data Sources

		$w = 200$ days			$w = 250$ days			$w = 300$ days		
		$h = 5$	$h = 10$	$h = 15$	$h = 5$	$h = 10$	$h = 15$	$h = 5$	$h = 10$	$h = 15$
	$h = 5$	1.000	1.000	1.000	0.978	0.978	0.978	0.959	0.959	0.959
$w = 200$	$h = 10$		1.000	1.000	0.977	0.977	0.977	0.958	0.958	0.958
	$h = 15$			1.000	0.977	0.977	0.977	0.958	0.958	0.958
	$h = 5$				1.000	1.000	1.000	0.986	0.986	0.986
$w = 250$	$h = 10$					1.000	1.000	0.986	0.986	0.986
	$h = 15$						1.000	0.986	0.986	0.986
	$h = 5$							1.000	1.000	1.000
$w = 300$	$h = 10$								1.000	1.000
	$h = 15$									1.000

(a) DY Spillover Index

		$w = 200$ days			$w = 250$ days			$w = 300$ days		
		$h = 5$	$h = 10$	$h = 15$	$h = 5$	$h = 10$	$h = 15$	$h = 5$	$h = 10$	$h = 15$
	$h = 5$	1.000	0.695	0.694	0.996	0.821	0.821	0.984	0.897	0.896
$w = 200$	$h = 10$		1.000	1.000	0.698	0.870	0.870	0.705	0.797	0.798
	$h = 15$			1.000	0.697	0.870	0.870	0.704	0.797	0.798
	$h = 5$				1.000	0.826	0.826	0.995	0.907	0.907
$w = 250$	$h = 10$					1.000	1.000	0.832	0.903	0.903
	$h = 15$						1.000	0.832	0.903	0.903
	$h = 5$							1.000	0.912	0.912
$w = 300$	$h = 10$								1.000	1.000
	$h = 15$									1.000

(b) KL Divergence Criterion

NOTE: The table reports balanced sample correlation coefficients for the DY spillover index and the Kullback Leibler divergence criterion as the window length is varied over $\tau = \{200, 250, 300\}$ trading days and the forecast horizon is varied over $h = \{5, 10, 15\}$ trading days.

Table 2: Sensitivity to the Choice of Window Length and Forecast Horizon

	Silverman	Gaussian	Epanechnikov	BGK
Silverman	1.000	0.963	0.957	0.950
Gaussian		1.000	0.997	0.923
Epanechnikov			1.000	0.912
BGK				1.000

(a) Uniform Norm

	Silverman	Gaussian	Epanechnikov	BGK
Silverman	1.000	0.997	0.997	0.991
Gaussian		1.000	1.000	0.994
Epanechnikov			1.000	0.994
BGK				1.000

(b) Hilbert Norm

	Silverman	Gaussian	Epanechnikov	BGK
Silverman	1.000	0.992	0.992	0.973
Gaussian		1.000	1.000	0.979
Epanechnikov			1.000	0.979
BGK				1.000

(c) KL Divergence Criterion

NOTE: The table reports the correlation between the Uniform Norm, Hilbert Norm and Kullback Leibler divergence criterion over our rolling samples using four different kernels: the Gaussian kernel with Silverman's rule of thumb bandwidth (Silverman); the Gaussian kernel with the asymptotically optimal bandwidth (Gaussian); the Epanechnikov kernel with the asymptotically optimal bandwidth (Epanechnikov); and the BGK kernel with a data-driven bandwidth (BGK). In all cases, the window length is $\tau = 250$ trading days and the forecast horizon is $h = 10$ trading days.

Table 3: Sensitivity to the Choice of Kernel

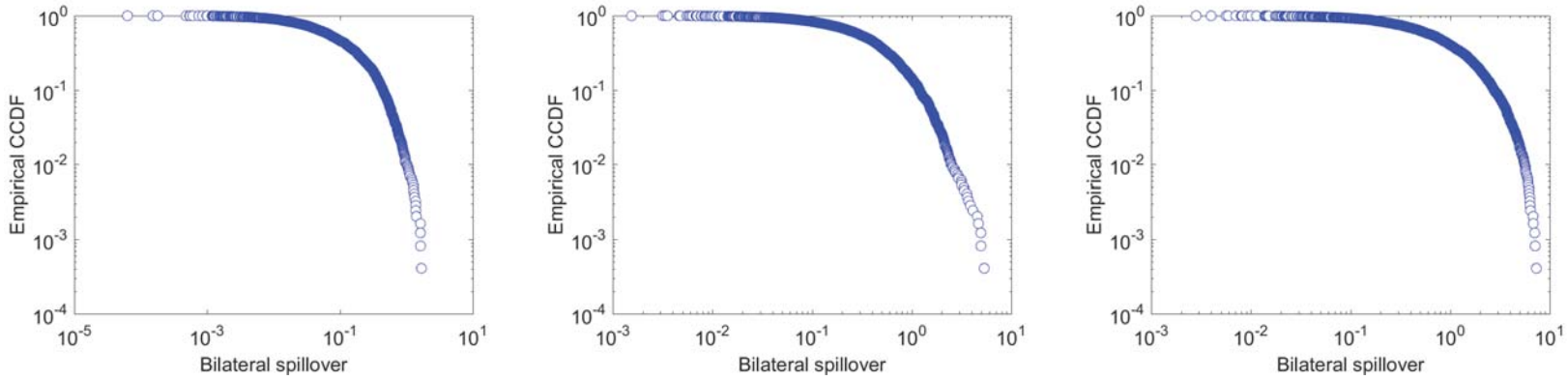

(a) Uncorrelated shocks (b) Weakly correlated shocks (c) Strongly correlated shocks

NOTE: The figure plots the empirical counter-cumulative distribution function (CCDF) for spillovers from a simulated DY network on a log scale under three different assumptions about the correlation of the shocks in the underlying VAR model. Simulations are based on the VAR(1) process $\boldsymbol{A}\boldsymbol{y}_t = \boldsymbol{B}\boldsymbol{y}_{t-1} + \boldsymbol{e_t}$ where $\boldsymbol{e_t} \sim IIN\left(\boldsymbol{0}, \boldsymbol{\Sigma}\right)$ assuming a cross-sectional dimension of $N = 50$. To obtain uncorrelated shocks, we set $\boldsymbol{A} = \boldsymbol{I}_N$ and $\boldsymbol{\Sigma} = \boldsymbol{I}_N$ and draw $\boldsymbol{B} \sim MN(\boldsymbol{0}, \boldsymbol{\Omega}_B)$ where $\boldsymbol{\Omega}_B = \tilde{\boldsymbol{B}}\tilde{\boldsymbol{B}}'$ and the (i,j)th element of $\tilde{\boldsymbol{B}}$ is drawn as $\omega_{\tilde{B},ij} \sim U(-1/2N, 1/2N)$ for $i, j \in \{1, 2, \ldots, N\}$. To obtain correlated shocks, we retain the same assumptions except that we now set the i-th diagonal element of $\boldsymbol{A}$ to $a_{ii} = 1$ $\forall i$ while we draw the a_{ij}'s from the multivariate normal distribution with mean $\boldsymbol{0}$ and covariance matrix $\boldsymbol{\Omega}_A = \tilde{\boldsymbol{A}}\tilde{\boldsymbol{A}}'$ where the (i,j)th element of $\tilde{\boldsymbol{A}}$ is drawn as $\omega_{\tilde{A},ij} \sim U(-c, c)$. For weakly correlated shocks we set $c = 1/2N$ and for strongly correlated shocks we use $c = 1/N$. In each case, we verify that the resulting VAR model is stationary and ergodic. Results are shown for a single representative draw. To account for the random variation across draws, Appendix Table A1 provides additional results based on 10,000 draws of $\boldsymbol{A}$ and $\boldsymbol{B}$.

Figure 1: Asymmetry of the Weighted Degree Distribution in the DY Framework

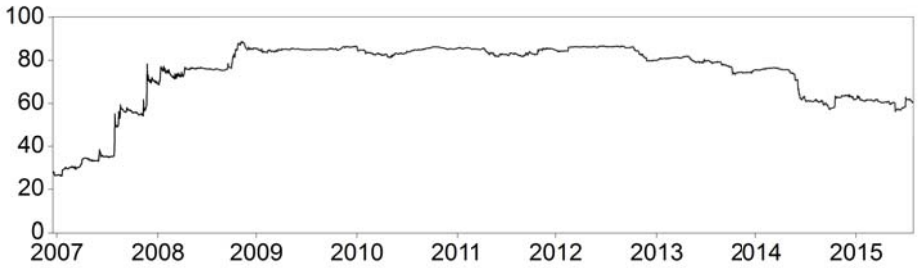

NOTE: The spillover index, $S^{(r,h)}_{y \leftarrow y}$, is computed according to equation (10) using a rolling window of $\tau = 250$ trading days and a forecast horizon of $h = 10$ trading days. The unit of measurement is percent. The dates shown on the horizontal axis correspond to the end of each rolling sample.

Figure 2: Evolution of the 10-days-ahead Spillover Index

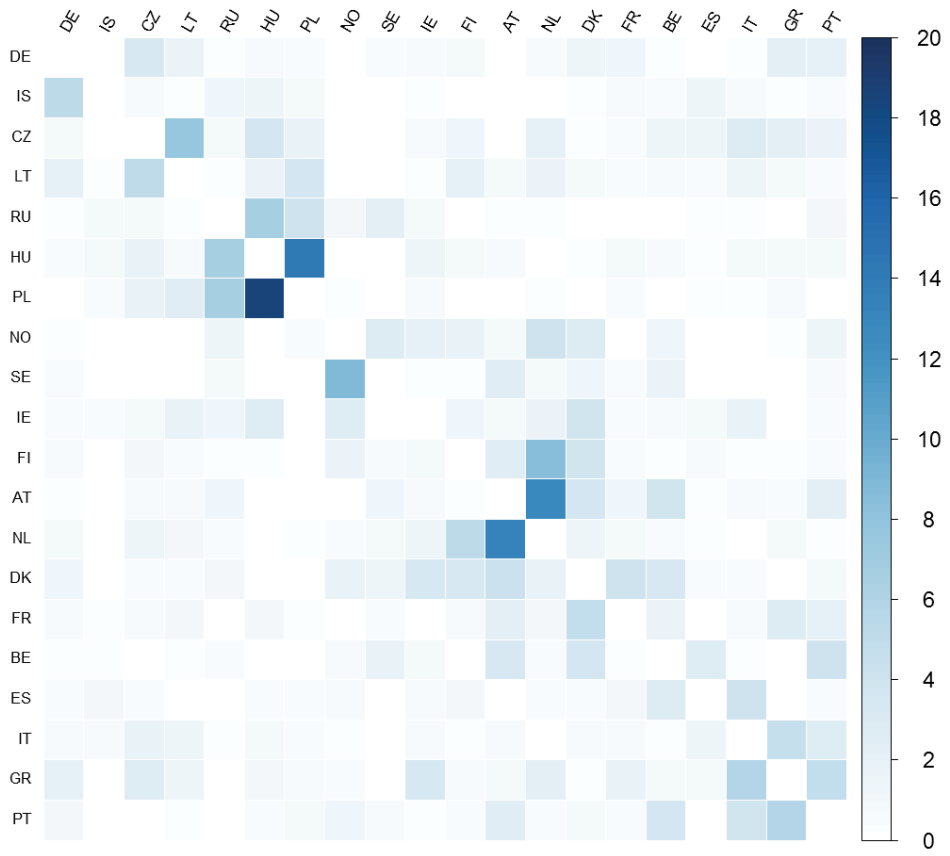

NOTE: The heat map summarises the ten-days-ahead spillover matrix for the first rolling sample, 02-Jan-2006 to 15-Dec-2006. Own-variable effects on the prime diagonal have been suppressed and the heatmap has been clustered according to a single linkage algorithm for clarity of presentation. To account for compositional changes between rolling samples, each element is adjusted by a scale factor of 20/23 according to the procedure described in Section II. The unit of measurement is percent.

Figure 3: Connectedness Heat Map for the First Rolling Sample (Benchmark Case)

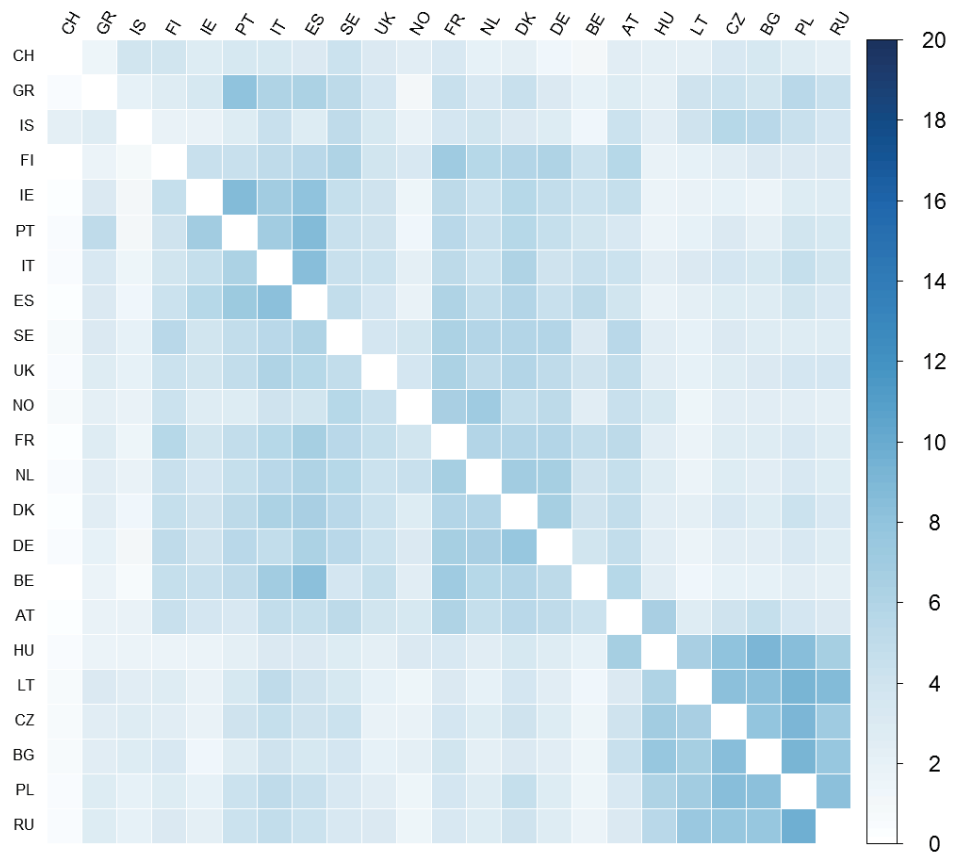

NOTE: The heat map summarises the ten-days-ahead spillover matrix for the sample spanning 22-Apr-2010 to 06-Apr-2011, the end point of which coincides with the Portuguese request for financial assistance. Own-variable effects on the prime diagonal have been suppressed and the heatmap has been clustered according to a single linkage algorithm for clarity of presentation. This sample contains all 23 sovereigns, so the scale factor described in Section II is equal to unity in this case. The unit of measurement is percent.

Figure 4: Connectedness Matrix after the Portuguese Request for Aid (06-Apr-2011)

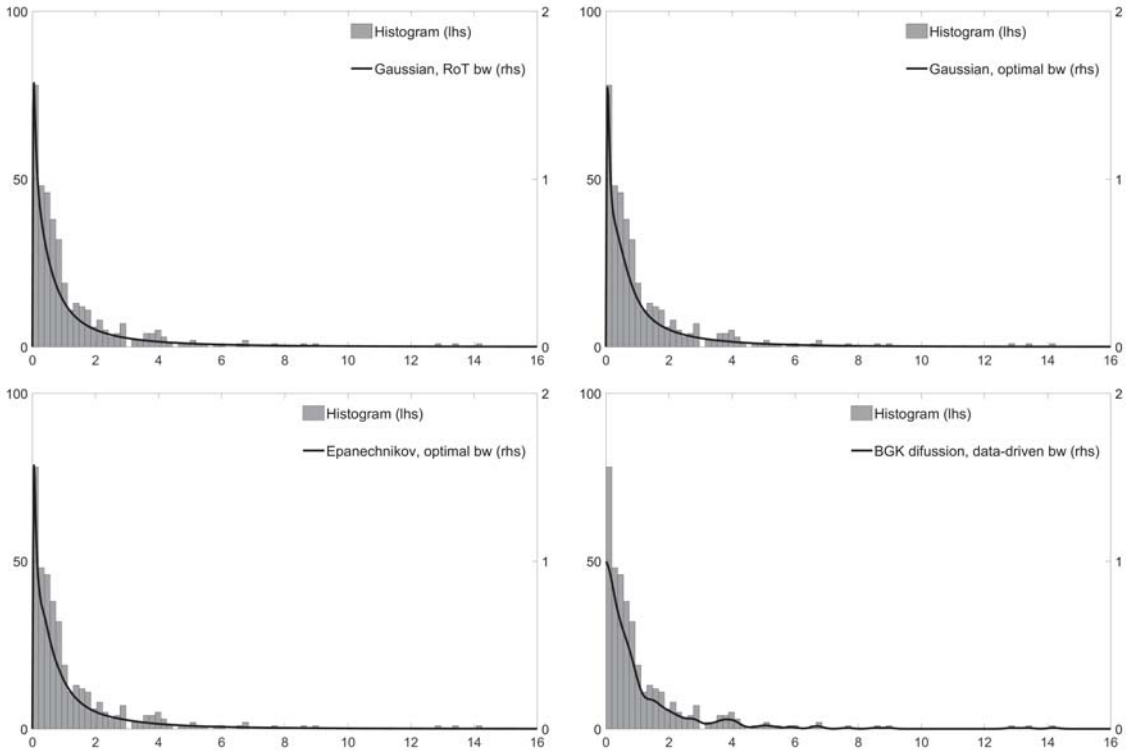

NOTE: The density plots are computed using the bilateral spillovers (i.e. the off-diagonal elements) of the ten-days-ahead spillover matrix for the first rolling sample, 02-Jan-2006 to 15-Dec-2006. The spillover density is estimated using four different implementations of the KDE: (i) the Gaussian kernel using Silverman's (1986) rule-of-thumb bandwidth; (ii) the Gaussian kernel using the asymptotically optimal bandwidth; (iii) the Epanechnikov kernel using the asymptotically optimal bandwidth; and (iv) the BGK adaptive approach using the data-driven bandwidth. The unit of measurement on the horizontal axis is percent.

Figure 5: Spillover Densities for the First Rolling Sample (Benchmark Case)

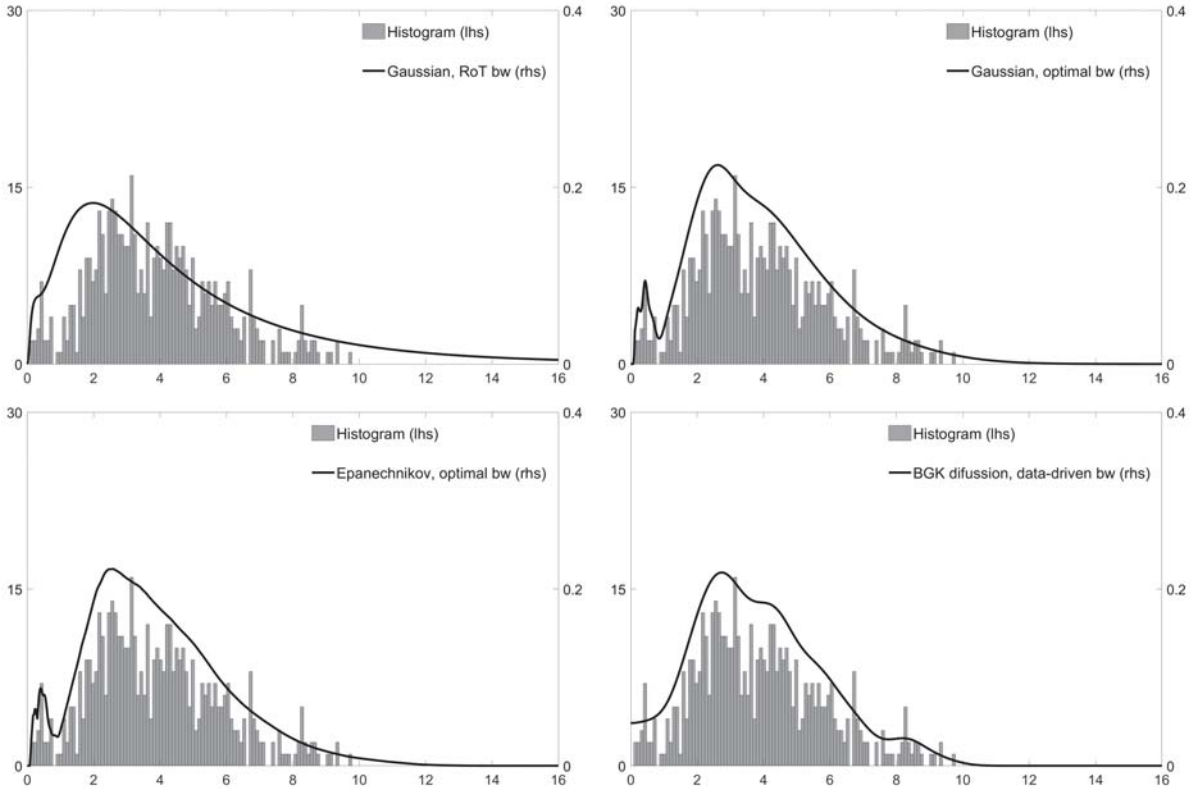

NOTE: The density plots are computed using the bilateral spillovers (i.e. the off-diagonal elements) of the ten-days-ahead spillover matrix for the sample spanning 22-Apr-2010 to 06-Apr-2011. The end point of this sample corresponds to Portugal's request for financial assistance. As in Figure 5, the spillover density is estimated using four different implementations of the KDE. The unit of measurement on the horizontal axis is percent.

Figure 6: Spillover Densities after the Portuguese Request for Aid (6-Apr-2011)

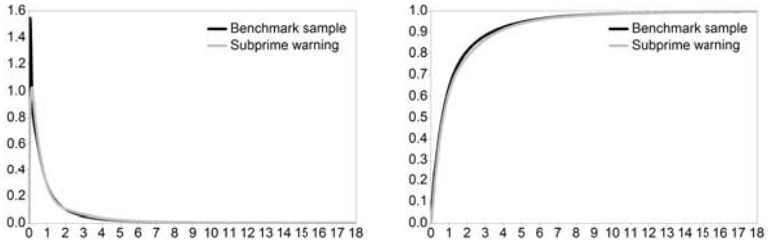

(a) Benchmark Sample and Bernanke's Subprime Warning

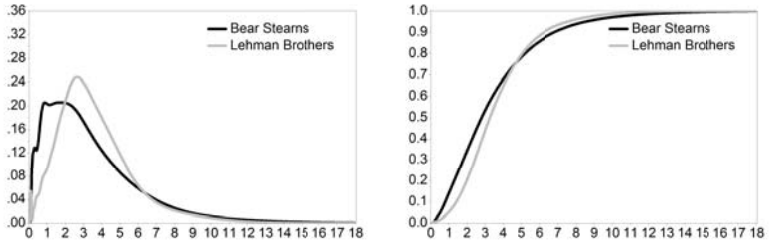

(b) Sale of Bear Stearns and Failure of Lehman Brothers

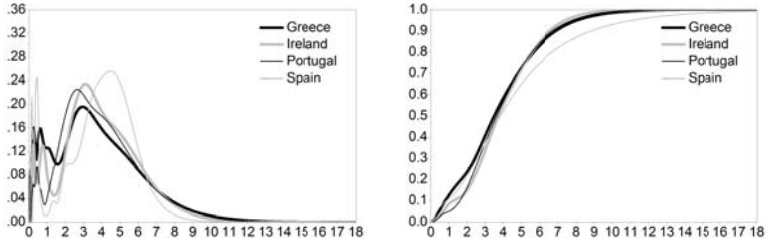

(c) GIIPS Sovereign Bailouts

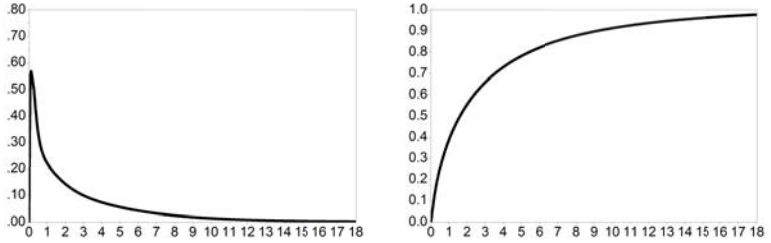

(d) Greek default on IMF repayments

Note: The figure presents PDFs (left side of each panel) and CDFs (right side) of the spillover density for the following events: the benchmark sample ending on 15-Dec-2006; Bernanke's warning of systemic risk in the subprime mortgage market on 06-Mar-2007; the acquisition of Bear Stearns by JP Morgan on 17-Mar-2008; the collapse of Lehman Brothers on 15-Sep-2008; the Greek request for aid on 23-Apr-2010; the Irish request for aid on 22-Nov-2010; the Portuguese request for aid on 06-Apr-2011; the Spanish request for aid on 25-Jun-2012; and the Greek default on its IMF debt repayments on 30-Jun-2015. If an event occurs on a non-trading day, the event date that we report refers to the next available trading day in our sample. The forecast horizon is $h = 10$ trading days in all cases and the unit of measurement on the horizontal axis is percent.

Figure 7: Changes in the Spillover Density, Selected Events

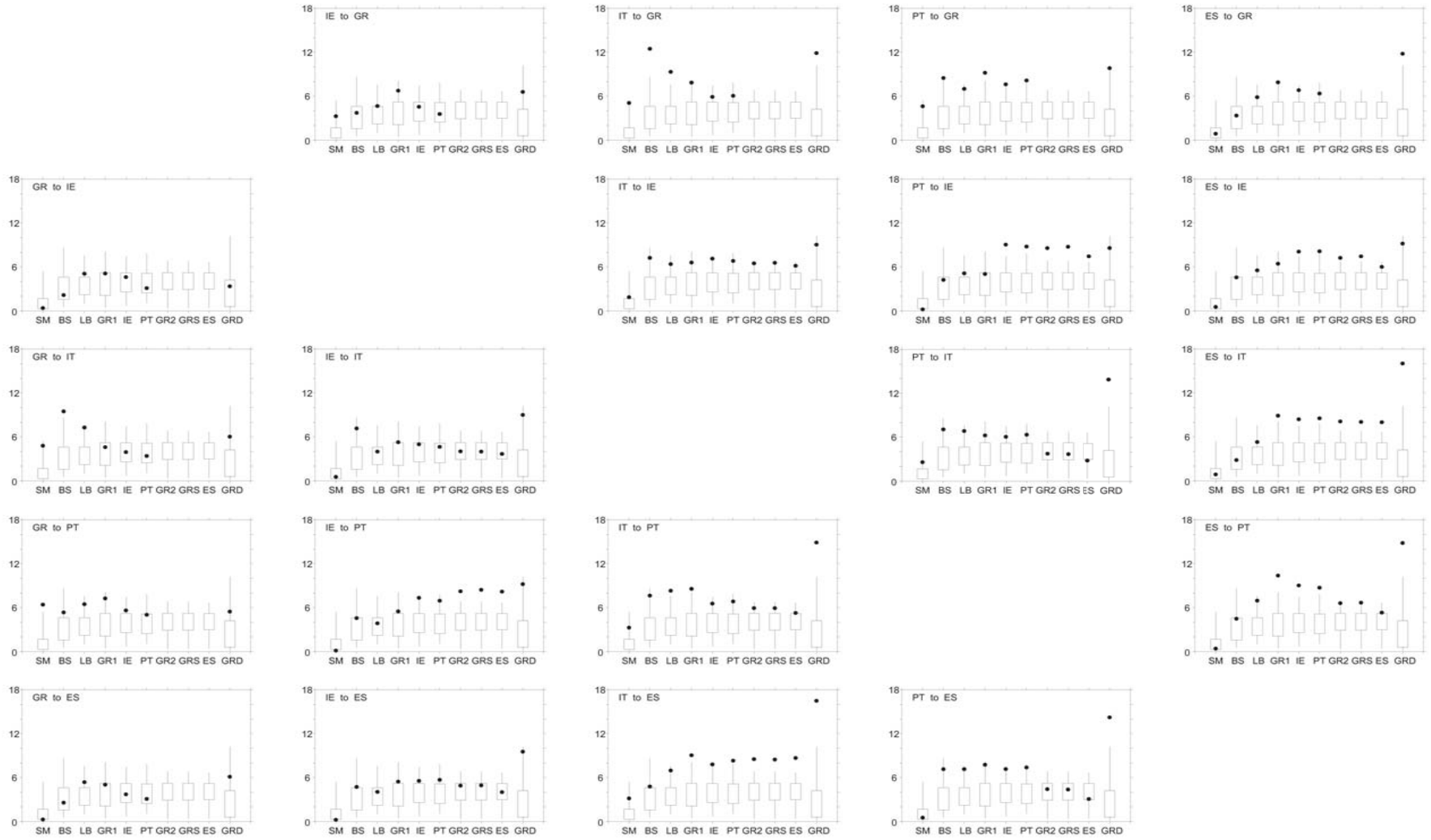

Note: The figure reports bilateral spillovers among the GIIPS for the following events: Bernanke's warning of systemic risk in the subprime mortgage market on 06-Mar-2007 (SM); the acquisition of Bear Stearns by JP Morgan on 17-Mar-2008 (BS); the collapse of Lehman Brothers on 15-Sep-2008 (LB); the Greek request for aid on 23-Apr-2010 (GR1); the Irish request for aid on 22-Nov-2010 (IE); the Portuguese request for aid on 06-Apr-2011 (PT); the agreement over the second Greek bailout on 21-Feb-2012 (GR2); the Greek debt-swap agreement on 09-Mar-2012 (GRS); the Spanish request for aid on 25-Jun-2012 (ES); and Greece's failure to meet its IMF payments deadline on 30-Jun-2015 (GRD). If an event occurs on a non-trading day, the event date that we report refers to the next available trading day in our sample. Missing points in the panels relating to Greece arise due to the lack of Greek CDS data between 15-Feb-2012 and 10-Jun-2013. For each event, the interquartile range of the spillover density is shown as a box and the 5-95% percentile range as whiskers. The vertical axis is in percent.

Figure 8: Bilateral Credit Risk Spillovers among the GIIPS

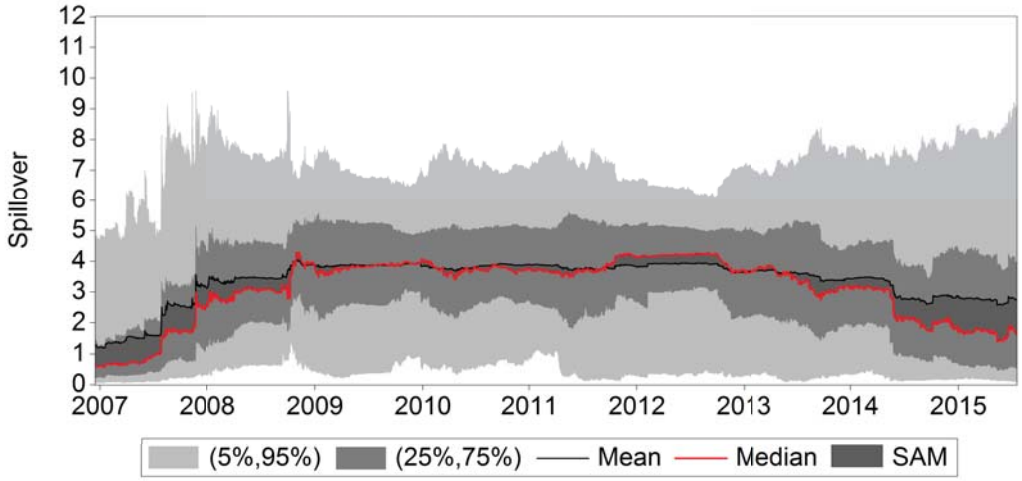

(a) Contour plot of the spillover histograms over rolling samples

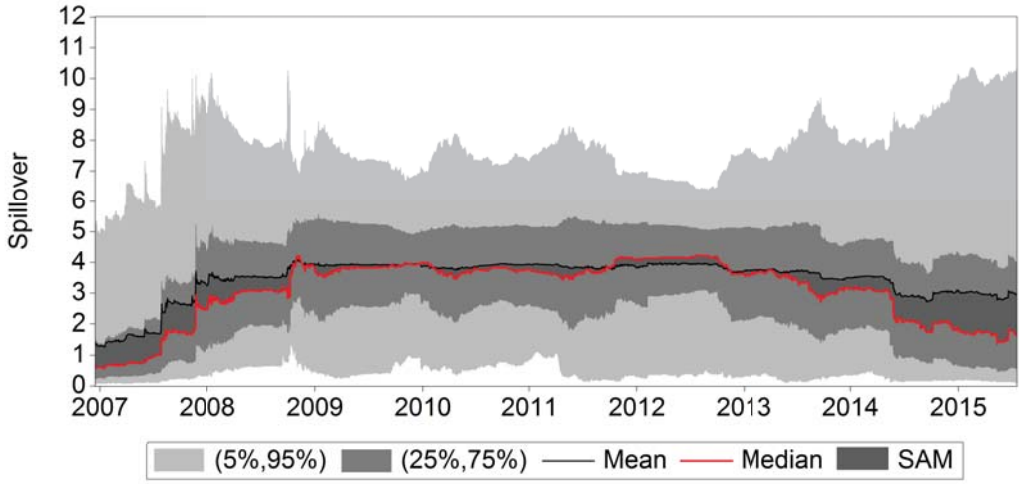

(b) Contour plot of the spillover densities over rolling samples

NOTE: Panels (a) and (b) present contour plots which trace the mean, the median, the spillover asymmetry measure (SAM) and selected percentiles of the spillover histogram and spillover density (respectively) over rolling samples. In each rolling sample, the spillover density is computed using the Gaussian kernel with the asymptotically optimal bandwidth. The window length is set at $\tau = 250$ trading days and the forecast horizon at $h = 10$ trading days. The unit of measurement on the vertical axis is percent. The dates shown on the horizontal axis correspond to the end of each rolling sample.

Figure 9: Comparison of the Spillover Density and the Spillover Histogram

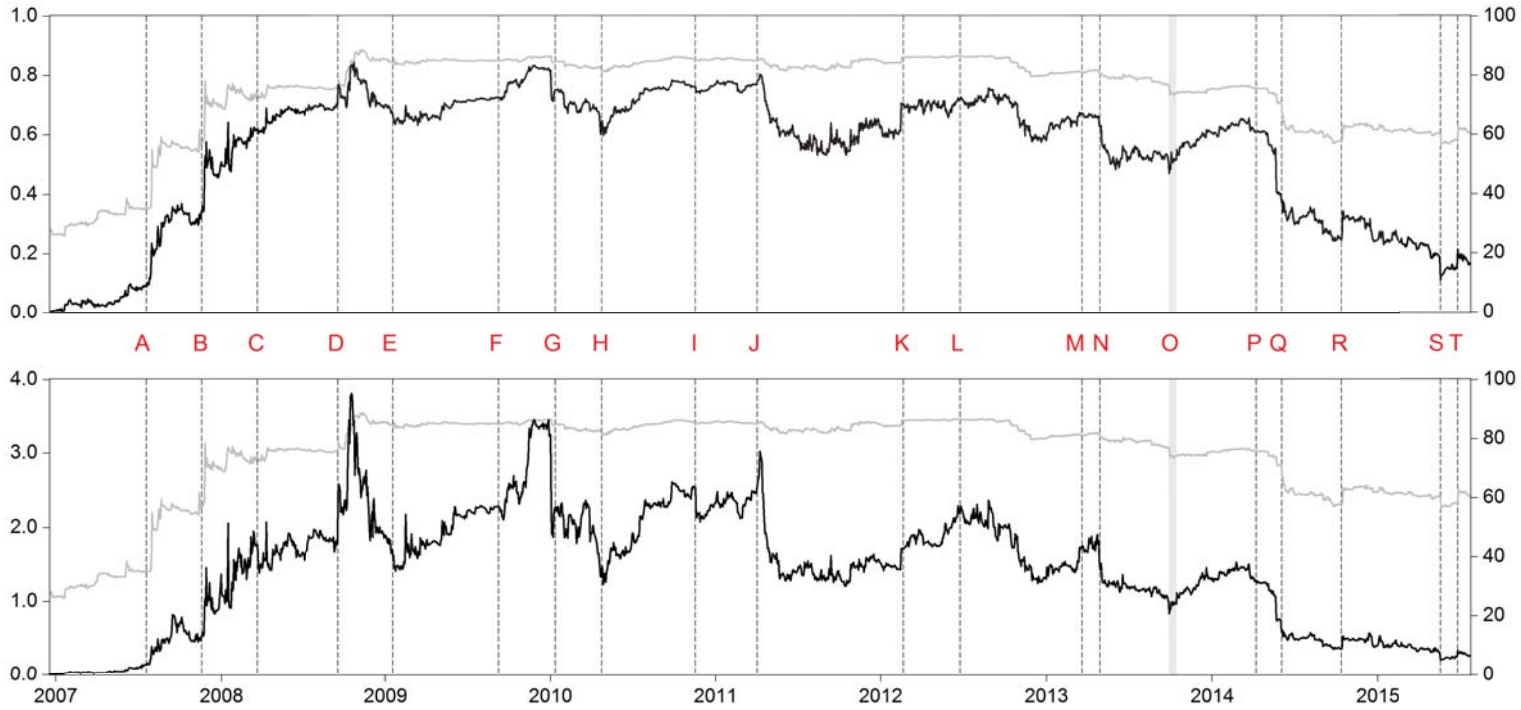

NOTE: The black lines represent the Hilbert norm (top panel) and the KLIC (bottom panel) which are plotted on the left axis. The gray line in each case is the DY spillover index plotted on the right axis. The spillover density is computed using the Gaussian kernel with the asymptotically optimal bandwidth and the density in the first rolling sample is used as the benchmark density, f_0. The window length is set at $\tau = 250$ trading days and the forecast horizon at $h = 10$ trading days. The dates shown on the horizontal axis correspond to the end of each rolling sample. Vertical lines/shading indicate the following events: (A) two Bear Stearns hedge funds collapse; (B) Bear Stearns is downgraded by S&P; (C) Bear Stearns is acquired by JP Morgan; (D) Lehman Brothers files for bankruptcy; (E) RBS reports record losses; (F) Greek parliament is dissolved; (G) European Commission releases a report on the falsification of Greek economic data; (H) Greece requests aid; (I) Ireland requests aid; (J) Portugal requests aid; (K) second Greek bailout; (L) Spain requests aid; (M) Cypriot bailout announced; (N) ECB cuts interest rates to a record low of 0.5%; (O) US federal government shutdown; (P) Greece returns to the bond market; (Q) ECB announces negative interest rate policy; (R) the October 2014 *flash-crash*; (S) Yellen discusses the case for a rate rise; (T) Greece misses its IMF payment deadline.

Figure 10: Measuring Changes in the Shape of the Spillover Density via Divergence Criteria

Appendix A: Additional Simulation Results

	Mean	Variance	Skewness	Kurtosis
Uncorrelated shocks				
Lower Decile	0.157	0.042	2.484	11.128
Median	0.165	0.047	2.751	13.820
Upper Decile	0.175	0.053	3.131	18.755
Weakly correlated shocks				
Lower Decile	0.443	0.189	1.825	7.248
Median	0.472	0.221	2.063	9.048
Upper Decile	0.508	0.264	2.402	12.385
Strongly correlated shocks				
Lower Decile	1.068	1.277	1.555	5.526
Median	1.188	1.522	1.867	7.218
Upper Decile	1.347	1.797	2.141	9.180

Note: All simulations are based on the VAR(1) process $\boldsymbol{A}\boldsymbol{y}_t = \boldsymbol{B}\boldsymbol{y}_{t-1} + \boldsymbol{e_t}$ where $\boldsymbol{e_t} \sim IIN\Big(\boldsymbol{0}, \boldsymbol{\Sigma}\Big)$ assuming a cross-sectional dimension of $N = 50$. To obtain uncorrelated shocks, we set $\boldsymbol{A} = \boldsymbol{I}_N$ and $\boldsymbol{\Sigma} = \boldsymbol{I}_N$ and draw $\boldsymbol{B} \sim MN(\boldsymbol{0}, \boldsymbol{\Omega}_B)$ where $\boldsymbol{\Omega}_B = \tilde{\boldsymbol{B}}\tilde{\boldsymbol{B}}'$ and the (i,j)th element of $\tilde{\boldsymbol{B}}$ is drawn as $\omega_{\tilde{B},ij} \sim U(-1/2N, 1/2N)$ for $i, j \in \{1, 2, \ldots, N\}$. To obtain correlated shocks, we retain the same assumptions except that we now set the i-th diagonal element of $\boldsymbol{A}$ to $a_{ii} = 1$ $\forall i$ while we draw the a_{ij}'s from the multivariate normal distribution with mean $\boldsymbol{0}$ and covariance matrix $\boldsymbol{\Omega}_A = \tilde{\boldsymbol{A}}\tilde{\boldsymbol{A}}'$ where the (i,j)th element of $\tilde{\boldsymbol{A}}$ is drawn as $\omega_{\tilde{A},ij} \sim U(-c, c)$. For weakly correlated shocks we set $c = 1/2N$ while for strongly correlated shocks $c = 1/N$. In each case, we generate 10,000 draws of $\boldsymbol{A}$ and $\boldsymbol{B}$ and verify that the resulting VAR model is stationary and ergodic. We then apply the Diebold-Yilmaz technique within each draw to estimate the set of $N(N-1)$ bilateral spillovers between variables. For each draw, we compute the sample mean, variance, skewness and kurtosis of the set of bilateral spillovers. The table reports selected percentiles of the empirical distributions of these four central moments obtained over the 10,000 draws.

Table A1: Evaluating the Shape of the Spillover Density by Simulation